Design of a Scalable and Optimized LED Grow-light System Driven by a High Efficiency DC-DC Power Converter

A THESIS SUBMITTED TO
THE FACULTY OF THE GRADUATE SCHOOL OF
THE UNIVERSITY OF MINNESOTA
BY

Omkar Joshi

IN PARTIAL FULFILLMENT OF THE REQUIREMENTS
FOR THE DEGREE OF MASTER OF SCIENCE

Adviser: Prof. Ned Mohan
May, 2019

Acknowledgements

Firstly, I would like to thank my adviser Prof. Ned Mohan for giving me the opportunity to work on this project and for his guidance towards completing it to satisfaction. Working on power electronics under the guidance of Prof. Mohan has been one of the major reasons to pursue MS in Electrical Engineering at University of Minnesota for me. His enthusiasm for the system design has been a primary force behind the success of this project.

I thank Prof. William Robbins and Prof. John Erwin in their capacity as members of the examining committee and their support in the project undertaken. I especially thank Prof. Erwin for his guidance on the horticulture aspects of LED Grow-lights and inspiring me to design this system after I worked on a similar system with PV-Battery integration last year.

I would also like to thank Abhijit Kshirsagar and Sreekanth Thamballa for their continued support, guidance and involvement throughout all the legs of this project and helping me with the other important aspects of the thesis.

Lastly I would like to express gratitude to Siddharth Raju for support with *Sciamble* products and my research group for all their help and making this a fun and memorable experience for me.

Dedication

To Aai, Baba, Guruji and Benjamin.

Abstract

Uncertainty in weather pattern adversely affects agriculture and results in food scarcity and food deserts in some regions of our planet. This has promoted research in the field of plant growth in controlled environment. The concept of artificial sunlight is significant in regions like Minnesota which don't get strong sunlight over the year and have an extremely cold climate. Modern LEDs called Grow-lights which have sufficiently high radiometric power output are replacing HID halogen lamps for such light. Despite the easy commercial availability of LED Grow-light systems, there is a need for scalable end-to-end system design with independent control over light spectrum channels so that it can used for any crop. An LED Grow-light system driven by an efficient buck based 4 channel DC-DC power converter with low current ripple which provides light from the PAR spectrum with controlled intensity was designed and simulated using *Matlab Simulink*. Hardware implementation of the system was done with the help of a micro-controller and *Sciamble Workbench* software developed at University of Minnesota.

Table of Contents

List of Tables

List of Figures

Chapter 1

Introduction

1.1 Structure of the Grow-light System

The proposed LED Grow-light system consists of 4 major parts – DC Power Source, DC-DC Power Converter, Current Controller and an LED Array. The following diagram shows the structure of the system:

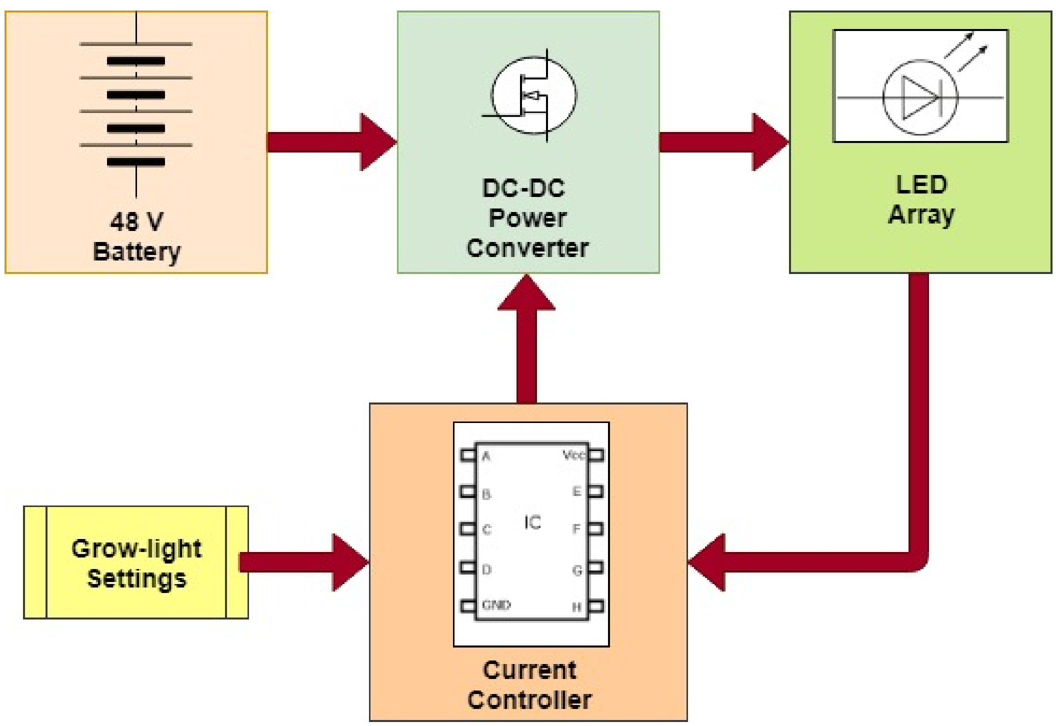

Figure 1.1: Block Diagram of Grow-light System

1.1.1 DC Power Source

The 48 V Lead-Acid Battery is the main source of power for the LED array. It can be easily built with 12 V cells and eliminates the requirement for another step down power converter to extract power from a source with a higher voltage such as the grid mains (110/230 V) or larger PV panels (50-100 V).

1.1.2 SIMO DC-DC Power Converter

The Single Input Multiple Output (SIMO) DC-DC power converter is a Silicon MOSFET based switched mode power supply that draws power from the 48 V battery and provides the current in 4 channels as required by the LED array to generate desired radiometric power output.

1.1.3 LED Array

Here, the LED Array has been built as a series-parallel combination of LED Grow-lights of 4 colors viz. Red, Deep Red, Blue and White. They serve as the main load for the DC-DC power converter. Controlled intensity of light of each of the mentioned 4 colors has a direct impact on the plants.

1.1.4 Current Controller

Radiometric power output of the LEDs is directly proportional to the current that they conduct. Hence, LED current can be measured and used as a feedback signal in order to control their radiometric power output and match it with the reference settings with the help of a current controller. Here, the Grow-light reference settings are power output based current values to be tracked by the controller.

The current controller is a Proportional-Integral (PI) control system in which reference input is the current settings given by the user, feedback signal is the measured LED current and the controller output is the duty ratio for Pulse Width Modulated (PWM) switching of the DC-DC power converter.

The output current of the DC-DC power converter is directly affected by the duty ratio of its PWM switching, the current controller generates the exact duty ratio needed to match the LED current with the reference given.

1.2 LED Grow-lights and Indoor Plant Growth

A grow-light is an artificial and generally electric source of light, designed to stimulate plant growth. Grow-lights are used in applications where there is either very less naturally occurring light or where supplemental light is required for plant growth. They are used for horticulture, indoor gardening, plant propagation and food production, including indoor hydroponics and aquatic plants. Although most grow-lights are used on an industrial level, they can also be used in households.

A range of bulb types can be used as grow-lights such as incandescent, fluorescent, high-intensity discharge (HID) and light-emitting diodes (LED). Indoor flower and vegetable growers typically use high-pressure sodium (HPS) and metal halide (MH) HID lights, but the LEDs are replacing metal halides due to their efficiency and economy [1].

LED grow-lights vary in color depending on the intended use since different light spectra have different effect on root formation, plant growth, and flowering. It has been shown that many plants grow better if given a specific color of light [2].

Modern technology has enabled to generate a specific spectrum of light of desired intensity that has a very good impact on the growth patterns and life cycle of plants. As a result, indoor plant growers have been able to achieve flowering and fruiting in plants at times very different than their natural flowering and fruiting season.

Apart from the flowers and fruits, lettuce is a plant widely grown in green houses these days. It has been experimentally proved that growth of lettuce, its life cycle and plant mass are affected by color of light it gets [3].

Conflict between the LED array configuration to suit the plants grown and the power input/output of the commercially available LED drivers poses the following challenges in designing LED Grow-light systems:

1. Design of LED drivers
2. Design of LED array

Since LED life is affected by ripple in current they draw, ultra-low current ripple in power output of the LED drivers is necessary for high luminous efficacy and reliability of LEDs [4]. Multi-channel LED driver design that gives independent control over the intensity of different colors of light is essential for future research in this field.

This project aims at conquering all the above challenges using a synchronous buck based 4 channel DC-DC power converter as an LED driver and an LED array design that gives customized light for any kind of plant.

Chapter 2

Illumination Requirements

Photosynthesis is the process by plants utilize sunlight to synthesize carbohydrates from carbon dioxide and water. In order to catalyze the process of photosynthesis, plants need sufficiently intense light so that the energy can be harnessed from it. Plants require light throughout their whole life-span from germination to flower and seed production. Three parameters of grow-lights used in greenhouse industries are relevant w.r.t. this: Light Spectrum, Light Intensity and Photo-period. All three parameters have different effects on plant performance.

2.1 Spectral Requirements

Out of the entire spectrum of sunlight, plants respond to only a small range of wavelengths. Since the other wavelengths aren't so significant for plant growth they can be skipped entirely or treated less significant when we design a Grow-light system. Following image explains the above [5]:

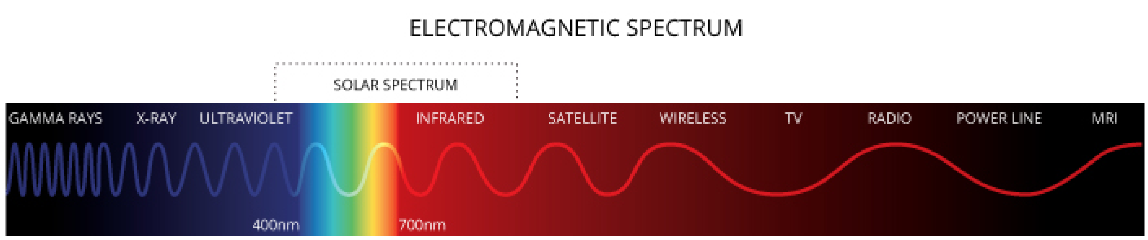

Figure 2.1: Electromagnetic Light Spectrum

2.1.1 PAR

Plants do not absorb all wavelengths of light (solar radiation), they are very selective in absorbing the proper wavelength according to their requirements. The most important part of the light spectrum is 400–700 nm which is known as photosynthetically active radiation [5] (PAR), this spectral range corresponds to approximately the visible spectrum of the human eye [1]. Figure 2.2 shows the position of PAR in the light spectrum.

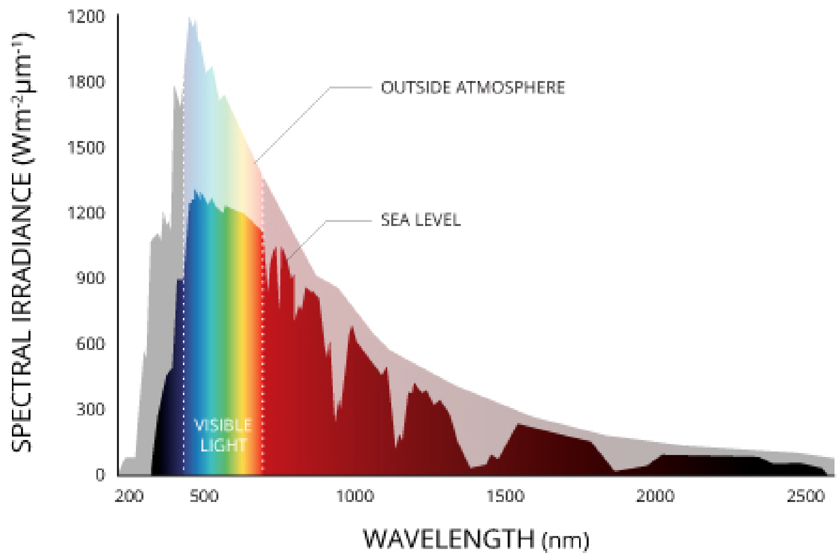

Figure 2.2: PAR $\approx$Visible Light

Different wavelengths of light have different effects on plants [6] which can be summarized as follows:

Color of Light	Wavelength (nm)	Effect on Plants
Ultra Violet	250-380	Long exposure is detrimental
Violet	380-445	Color, Taste and Aroma
Blue-Green	445-570	Growth and Maturity
Yellow	570-590	Long exposure slows down growth
Red	590-720	Vegetation and Plant Mass
Far Red	720-1000	Flowering and Reproduction

Table 2.1: Effects of colors of light on plants

Hence when LED Grow-lights are used for generating PAR, the intensity of specific colors of light can be adjusted to achieve desirable growth and changes in plants.

2.1.2 Red/Far Red Ratio

One of the crucial factors affecting plant growth is the ratio of Red to Far Red light (R/FR) in the composition of PAR incident on the plants that are grown in controlled environment. Phytochrome is a complex of pigments that occurs in two basic kinds: one that responds to red light (Pr) and another that responds to far red light (Pfr). Depending on the light frequencies that they absorb the most (even though the other frequency will also activate it and blue light too), the two pigments generally convert back and forth, with Pr converting to Pfr with red light and vice versa (although some forms of Pr/Pfr lose the ability to reconvert depending on the amount of light, the intensity, or the quality of the light received). The active form, which triggers responses such as flowering, is Pfr. Red light exerts the biggest influence on photomorphogenesis (the effect of light on plant development) and far red light can sometimes reverse Pfr responses [7].

This is because the plant senses the change through the ratio difference between red light and far red (or no light), and begins to change its physiology from a state of vegetative growth to floral growth. While the plant is receiving light, the ratio of Pr to Pfr (Pr: Pfr) is approximately in equilibrium (in fact, Pfr is slightly higher). Pr is converted to Pfr by red light and Pfr is converted back to Pr by far red light. As the sun sets, the amount of far red light exceeds the amount of red light and the levels of Pr increase, resulting in a slightly higher concentration of Pfr and a lower concentration of Pr. Following image shows the effect of different R/FR ratios ranging from 0.5 to 10 on *Eustoma grandiflorum (Raf.) Shinn*:

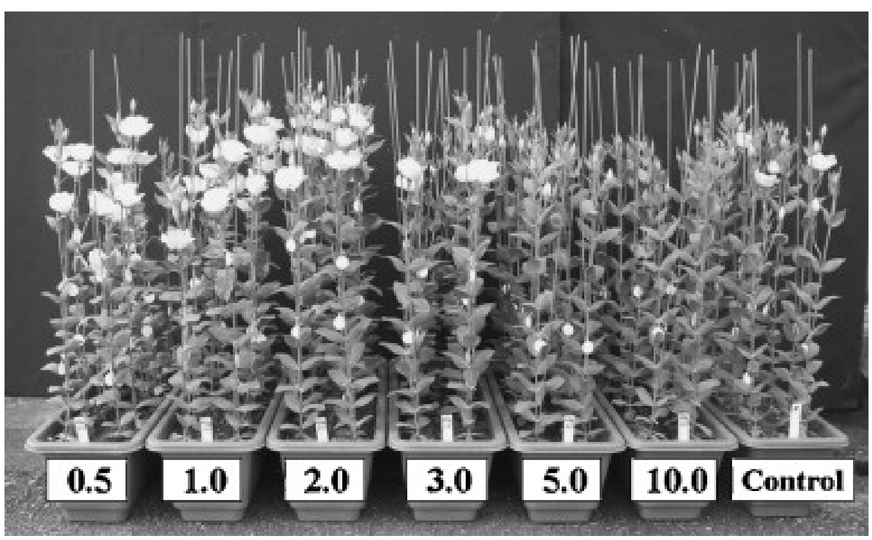

Figure 2.3: Effect of R/FR Ratios on *Eustoma grandiflorum (Raf.) Shinn* [8]

2.2 Intensity Requirements

Considering that each photon is capable of catalysing a particular step of the photosynthesis reaction, the incident radiation on plants is measured in the number of photons falling on the plant per unit area per unit time. Intensity of light has a huge impact on plants with vegetative growth. For example, Lettuce. After the leaves grow and become thick and wide enough, they shade the rest of the plant. Hence the intensity of light generated by Grow-lights has to be controlled through all the stages of plant growth.

2.2.1 Incident Energy - PPFD

Photons directly represent unit elements of light. Energy of a photon is given by the equation:

$$E = \frac{hc}{\lambda} \tag{2.1}$$

where E is the energy of photon (J), h is the Planck's constant (6.63×10^{-34} Js), c is the speed of light (3×10^{8} m/s) and λ is the wavelength of light. From above, the unit of measuring PAR can be deduced easily. A commonly used unit for measuring PAR is Photosynthetically Active Photon Flux Density (PPFD) and is defined as micro-moles of photons per square meter per second ($\mu mol/m^2s$). It has been observed that plants can tolerate PPFD as high as 600-800 $\mu mol/m^2s$ depending on how long the radiation is incident on them.

2.2.2 Photo Period

Photoperiod refers to the time that a plant is exposed to light in a 24 hour period. Many types of plants require certain lengths of light exposure to enter various life cycle stages. Growers frequently control the photoperiod in a plant's life cycle through the use of grow lights to encourage the plant's vegetative state, early flowering, bud phase, and ultimate harvest. Some plants also respond favorably to a longer than natural photoperiod by producing a more abundant harvest yield.

Some plants are considered long-day plants. Long-day plants require days that are longer than their critical day length time to flower. Short-day plants will flower on shorter day lengths. In the middle, there are day-neutral plants, requiring equal amounts of light and darkness.

2.2.3 Daily Light Integral

Daily Light Integral (DLI) refers to the rate at which PAR is delivered to plants in a 24 hour period [9]. DLI is normally defined as moles of PAR photons delivered to the plants in a day. DLI is calculated as follows:

$$DLI(mol/day) = PPFD(\mu mol/m^2 s) \times Photoperiod(hours) \times \frac{3600}{10^6} \tag{2.2}$$

Following table shows the recommended DLI for different types of plants with 8-12 hours of photoperiod:

Plant Type	**Recommended D.L.I. (mol/day)**
Herbs and Leaves	15-20
Flowers and Fruits	25-30
Cannabis	35-40

Table 2.2: D.L.I. for Different Plants

Tomatoes, Spinach and Lettuce were the plants primarily referenced as test subjects for the designed grow-light system. One of the main goals for the system design was also to make it scalable w.r.t size and radiometric power rating. Lettuce was considered to set the reference for minimum DLI needed for any kind of plant grown with grow-lights since it can grow with the smallest DLI and a long photoperiod since it is a long day plant.
The minimum recommended DLI for Lettuce is 13 mol/day. With 18 hour photoperiod and 200 $\mu mol/m^2 s$ of PPFD, the DLI output of the system can be calculated using equation (2.2) as follows:

$$DLI Output of System = 200 \times 18 \times \frac{3600}{10^6} = 12.96 \approx 13 mol/day \tag{2.3}$$

Setting 200 $\mu mol/m^2 s$ as the base PPFD rating of the system enables us to scale it to a higher PPFD capacity if needed which can be achieved just as a multiple of 200 $\mu mol/m^2 s$. It not only makes the PPFD scalable but also makes the electrical properties of the system easier to tweak since then it is only a question of series-parallel combination of blocks where each block is a system design discussed in the thesis. Scalability of PPFD and control over the photoperiod enables us to use this system with equal efficacy for long and short day plants.

Chapter 3

Performance of Existing LED Emitters

After the light intensity, spectrum and photoperiod have been determined for the range of applications, it is possible to design an LED panel that can cater to the entire range of output demand. However, before this can be done, it is important to characterise the commercially available LEDs for their PPFD output as a function of current. An experiment was performed to study the above mentioned characteristics of a commercially available LED panel and inferences were drawn which serve as a reference for the system design.

3.1 Description of Experiment

1. A 2 sq.ft. LED Grow-light panel manufactured by *GrowFilm LLC* was used to measure PPFD and emission efficiency of the panel for various current inputs and panel heights; and also to study the effect of reflectors on distribution of light intensity.

2. The 2 sq.ft LED Grow-light panel consists of a total of 144 LEDs comprising of Red, Deep Red (FR), Blue and White light emitting LEDs manufactured by *Everlight Americas Inc.*.

3. The panel was subjected to electric current input of 0.5-2 A in steps of 0.5 A and was placed at a height of 1, 1.25 and 1.5 ft. respectively for test purposes. A PAR meter was used to measure the PPFD at 36 positions in a 2 dimensional 6 x 6 grid.

3.2 PPFD Measurement Results

Following are the characteristics of the LED panel that were studied in this experiment:

1. PPFD versus current drawn
2. PPFD v/s current and panel height without reflectors
3. PPFD v/s current and panel height with reflectors
4. PPFD/A versus current for 2 panels

Following results display the above characteristics:

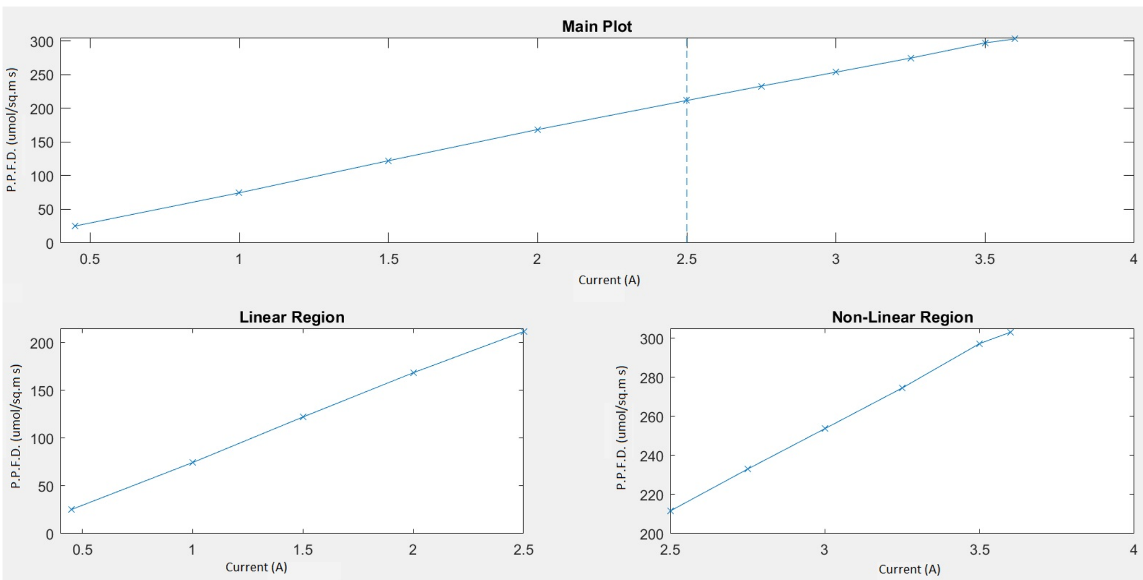

Figure 3.1: PPFD ($\mu mol/m^2 s$) versus current drawn (A)

Note: For figure 3.2 and 3.3, columns correspond to current values (0.5-2 A) and rows correspond to panel heights (1-1.5 ft).

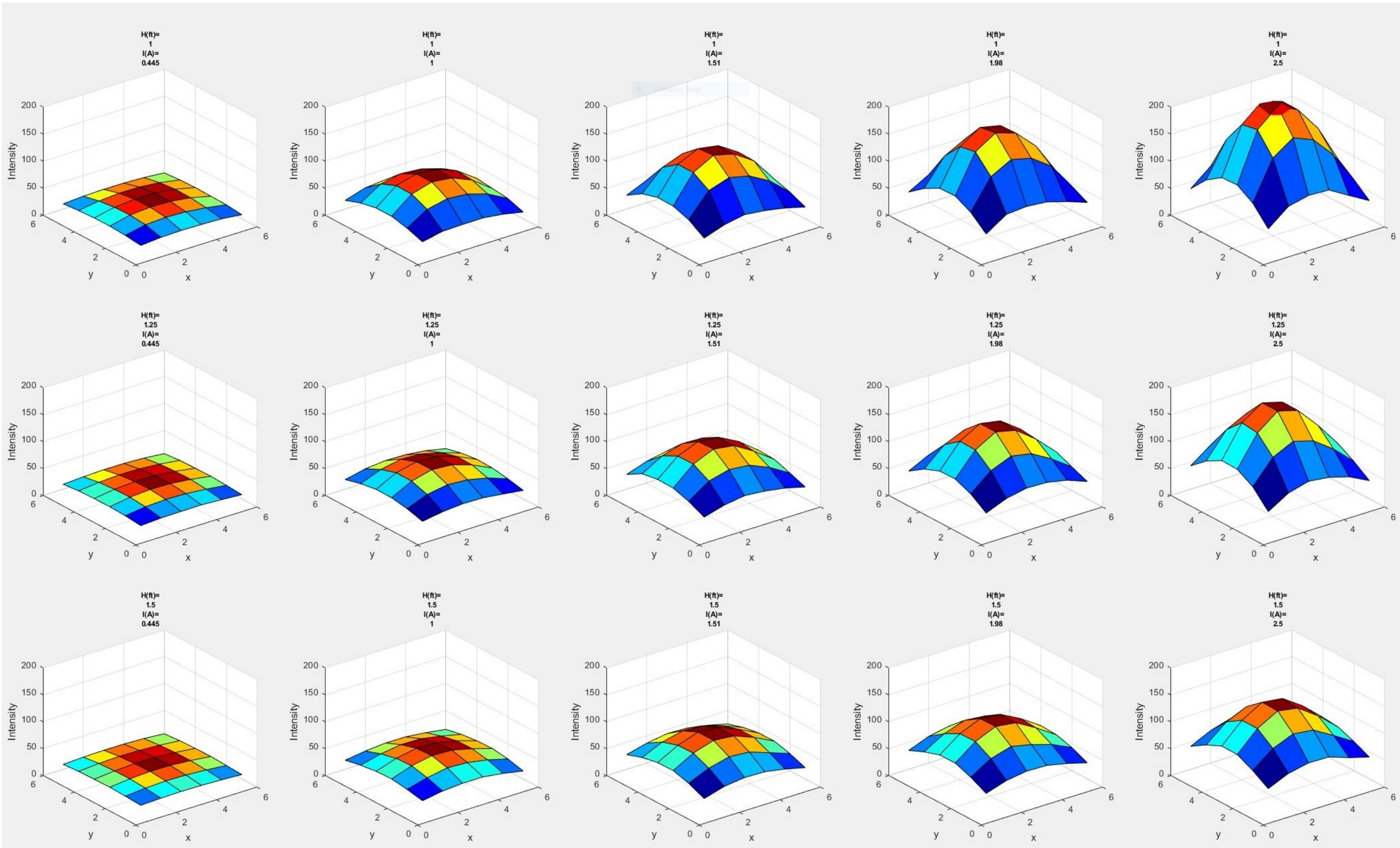

Figure 3.2: PPFD ($\mu mol/m^2s$) versus Current Drawn (A) and Panel Height (m) without reflectors

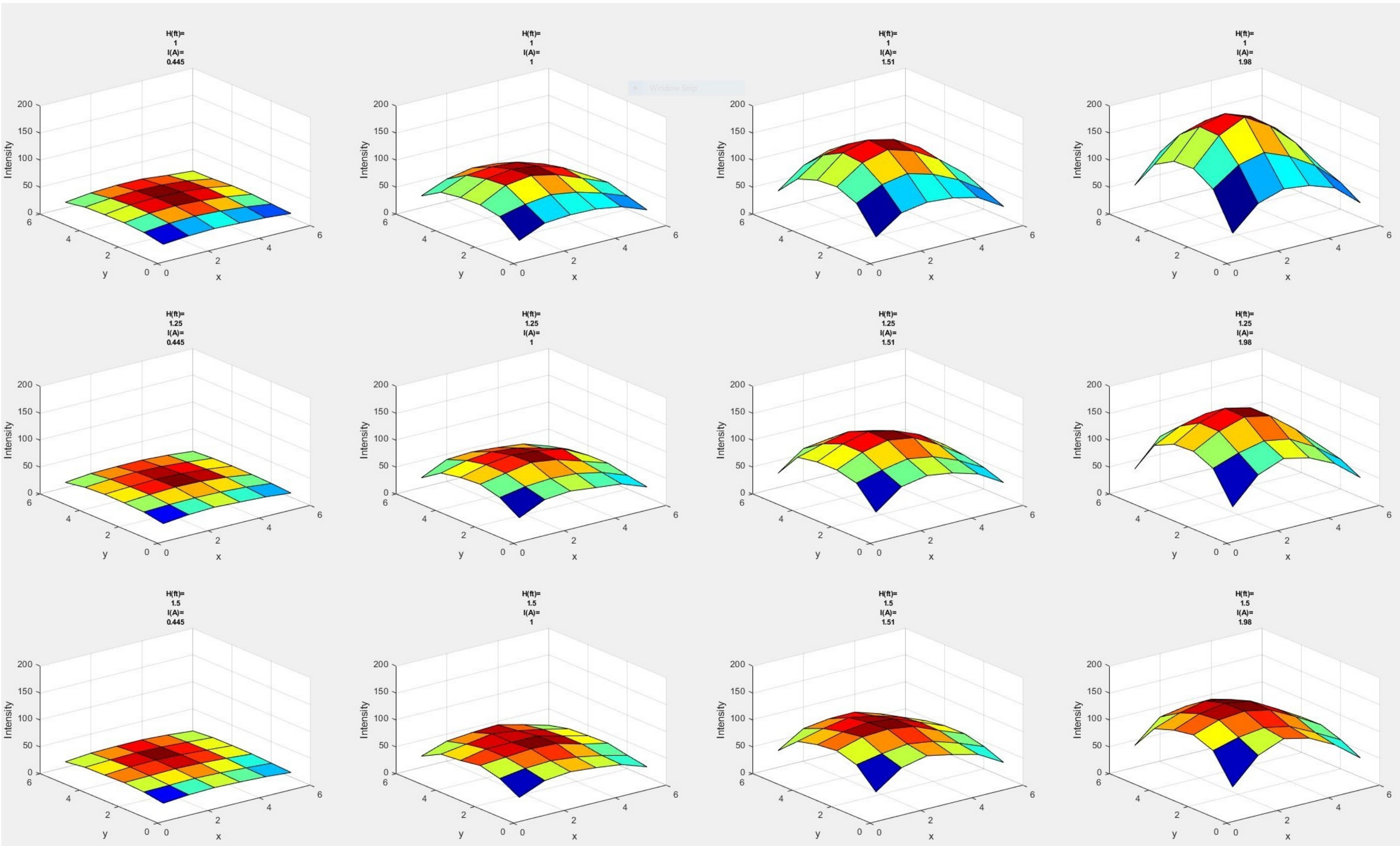

Figure 3.3: PPFD ($\mu mol/m^2 s$) versus Current Drawn (A) and Panel Height (m) with reflectors

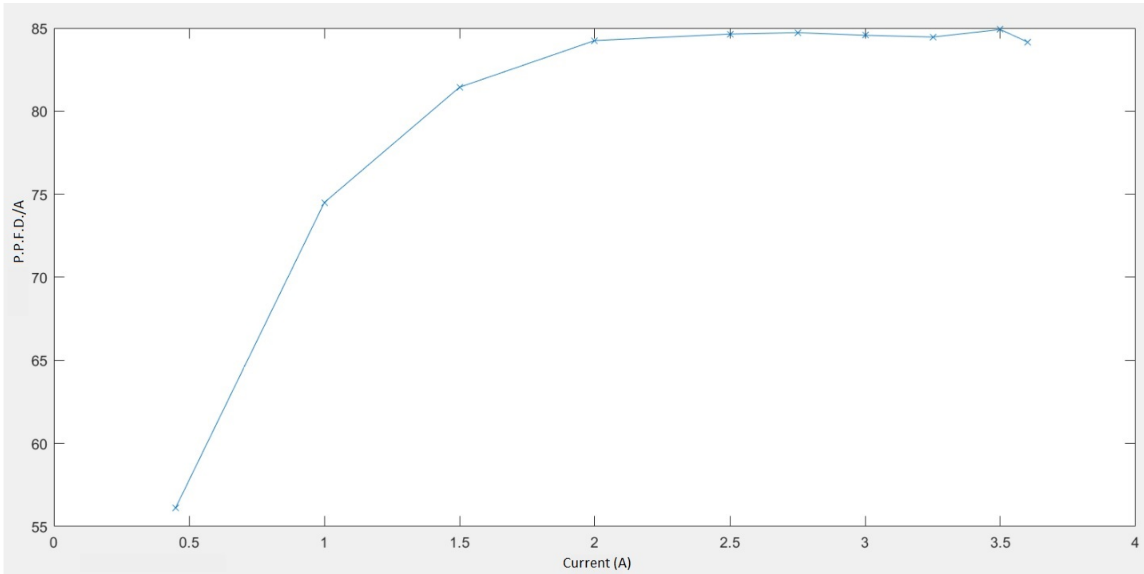

Figure 3.4: PPFD/A ($\mu mol/m^2 s$/A) versus current drawn (A)

3.3 Inferences

1. The intensity of light becomes more uniform when reflectors are used.

2. Intensity of light becomes less uniform with increase in panel height.

3. The radiometric power output of LED panel varies almost linearly with the current drawn.

4. The PPFD/A obtained increases exponentially up to a point and then drops beyond it since excess electric current generates more heat than normal. Thus, the highest efficiency of the panel is obtained at the electric current of 2.5 A.

Chapter 4

Design of LED Array

The LED panel used for the above experiment gives a maximum PPFD of 300 $\mu mol/m^2s$ and consists of 144 LEDs with the following composition:

Color of Light	**No. of LEDs**	% **Composition**	PPFD Contribution ($\mu mol/m^2s$)
Red	100	69	210
Deep Red	20	14	42
Blue	18	12.5	40
White	6	4.5	18

Table 4.1: Composition of Existing LED Panel

4.1 Design Criteria

As discussed in section 2.2.3, the rated PPFD for system design has been set to 200 $\mu mol/m^2s$ in order to make the system scalable. Since the system also has to cater to both kinds of plants viz. flowering and vegetative, control over the R/FR ratio in illumination is desirable.
Thus, following are the main constraints on the design of LED array:

1. Maximum PPFD capacity of 200 $\mu mol/m^2s$

2. Flexible R/FR ratio ranging from 0.5 to 10

4.2 Color Composition Design

With the maximum of 200 $\mu mol/m^2s$ of PPFD capacity and to accommodate the full specified range of R/FR ratios, the number of LEDs of Red and Deep Red type is adjusted to the maximum number needed for generating equivalent PPFD ($\mu mol/m^2s$) for each R/FR ratio. Following table shows the composition of LEDs chosen to satisfy both the above design constraints:

R/FR $\approx$ 10		**R/FR $\approx$ 0.5**		**Chosen PPFD**
Color of Light	**PPFD**	**Color of Light**	**PPFD**	
Red	156	Red	60	156
Deep Red	20	Deep Red	120	120
Blue	12	Blue	10	12
White	12	White	10	12

Table 4.2: Composition of Colors for PPFD and R/FR Ratio

Generally, an LED color composition having more contribution from Red and Deep Red light is preferred. Keeping almost the same composition as the panel used for testing, the number of LEDs can be calculated proportionally for the above configuration as follows:

Color of Light	**PPFD ($\mu mol/m^2s$)**	**No. of LEDs**
Red	156	80
Deep Red	120	60
Blue	12	12
White	12	8

Table 4.3: Number of LEDs w.r.t. Light Composition

Example calculation of number of LEDs needed for satisfying the PPFD and R/FR ratio constraints:

- Consider Red light. The existing panel with maximum PPFD 300 $\mu mol/m^2s$ has its PPFD contribution equal to 210 $\mu mol/m^2s$.

- With the new PPFD maxima of 200 $\mu mol/m^2s$, the contribution of Red light comes down proportionally to 140 $\mu mol/m^2s$. But to get say an R/FR ratio $\approx$ 10, the contribution is 156 $\mu mol/m^2s$ and for an R/FR ratio of $\approx$ 0.5 it is 60 $\mu mol/m^2s$ keeping the number of Red and Deep Red LEDs proportionally the same.

- Chosing 156 $\mu mol/m^2s$ as the PPFD contribution for more flexibility on R/FR ratio, the proportional number of Red LEDs can be calculated as 80 to keep the total number of LEDs an even number.

Chapter 5

Circuit Design

The existing *Invertronics* LED driver used for driving the LED panels used in the discussed experiment requires 127-250/300 V DC power source and provides 18-25 V 0-5.6 A current to the LED loads driven by it. However, it has a single channel output and thus fails to provide control over intensity of different colors of light which is one of the main goals of this project.

5.1 Design Criteria

Following are the design constraints for the DC-DC power converter to be designed and used as an LED driver:

1. **Current Ripple Tolerance**
   Ripple in the current supplied to the LEDs not only makes them flicker affecting their radiometric output but also takes a toll on their life. It has been proven that the luminous efficacy of LEDs decreases with increase in the current ripple [4]. Thus, in order to minimize LED ageing and avoid drop in luminous efficacy, the LED driver has to supply current with minimal ripple. Here 10% peak to peak ripple current has been set as the highest tolerance.

2. **Voltage and Current Ratings**
   Every LED has a forward voltage. Thus, a configuration of N series and M parallel connected LEDs can achieve a desirable output voltage. One of the important criterion in selecting the output voltage is to choose it such that the DC-DC converter operates in CCM (continuous Conduction Mode) at all times. The LEDs are binned with characteristic forward current, radiometric power and forward voltage.

Thus a suitable N x M array of LEDs can be designed to satisfy the output voltage and power output constraints. With a high input voltage, another step-down DC-DC converter is needed to bring the voltage down to a controllable level keeping the main power converter in continuous conduction mode since the output voltage is fairly small even with a large value of N. An input supply voltage of 48 V DC has been chosen here since this will allow the LEDs to be powered off a standard lead acid battery stack, eliminate the need for an additional power conversion stage and serve fairly good on the source stiffness and input current ripple tolerance fronts. The battery can be supplied by a grid facing converter and/or PVs based on the application.

3. **Choice of DC-DC Converter Topology**
   Since the main power converter has to step down voltage and provide output current with minimal ripple, a buck converter based topology has been chosen since it has an inductor on the load side which inherently suppresses ripple current.
   There are 2 choices in terms of design of the buck converters here. If a normal asynchronous buck converter with a freewheeling diode is used, switching loss is considerable but the cost and complication of an isolated high-side switch driver can be avoided by placing the switch on low voltage side. However, if a synchronous buck converter is used in CCM, switching loss can be eliminated on one switch and the gate drive can be selected as a single chip drive. Considering feasibility of the converter, a synchronous buck converter based topology is designed here.

5.2 LED Array and Forward Voltage Selection

5.2.1 LED Load Voltage Rating

The LEDs can be ordered from a variety of forward voltage (V_f) bins for each emission wavelength. The forward drop in each bin has a range of 0.1 V which makes it possible to have LED strings with very closely matched forward voltages. This ensures that the parallel strings share equal forward current. Based on the available forward voltage bins, we have designed optimal N x M LED arrays for each color.
While designing the LED array with series parallel connection of LEDs, it is important to achieve the output voltage which keeps the converter in CCM all the time. For buck converter the PWM duty ratio D is defined as ratio of output voltage to input voltage.

Here, the input voltage is 48 V. For CCM operation the duty ratio has to be greater than 0.5 i.e. the output voltage here has to be greater than 0.5 x 48 = 24 V. An ideal duty ratio for CCM is 0.6.

5.2.2 LED Forward Voltage Selection and N x M configuration

Based on the datasheets of LEDs from *Everlight Americas Inc.*, for the required PPFD, every Red and Deep Red LED should carry 150 mA of forward current (I_f) and every Blue and White LED should carry 180 mA of forward current. Following table summarizes the choice of bin for forward voltage (V_f) (V) and N x M configuration of LEDs:

Color of Light	V_f **(V)**	I_f **(mA)**	**N**	**M**	V_o **(V)**	I_o **(A)**	**No. of LEDs**	D
Red	1.9	150	16	5	30.4	0.75	80	0.633
Deep Red	2	150	15	4	30	0.6	60	0.625
Blue	3.4	180	9	2	30.6	0.36	18	0.638
White	3.4	180	9	2	30.6	0.36	18	0.638

Table 5.1: N x M Configuration of LEDs

Here, V_o and I_o are the total output voltage and output current respectively for a channel of the DC-DC power converter and D is the duty ratio for PWM switching. As the above table shows, the duty ratio achieved for each DC-DC power converter channel corresponding to a color in LED array is nearly 0.6 and can be considered close to ideal.

5.3 SIMO DC-DC Power Converter Topology

A buck converter based power converter topology has been chosen since it has continuous current on the load side which when combined with high-frequency (50 kHz) switching, leads to very low ripple in the current drawn by the LEDs. Efficiency is further improved by using a MOSFET based synchronous buck converter driven by a single chip gate driver with a boot-strapped high side drive to keep cost and complexity low.

The topology comprises of 4 synchronous buck converters - one for each channel of LEDs, connected in parallel configuration across the same 48 V DC power source. Current reference based PWM switching of the high-side and low-side switch in each channel results in a voltage step down and supply of current with a peak to peak ripple under 10%.

Following figure shows the Single Input Multiple Output (SIMO) synchronous buck-based DC-DC power converter topology designed to be used as an LED driver with independently controlled output current on each channel:

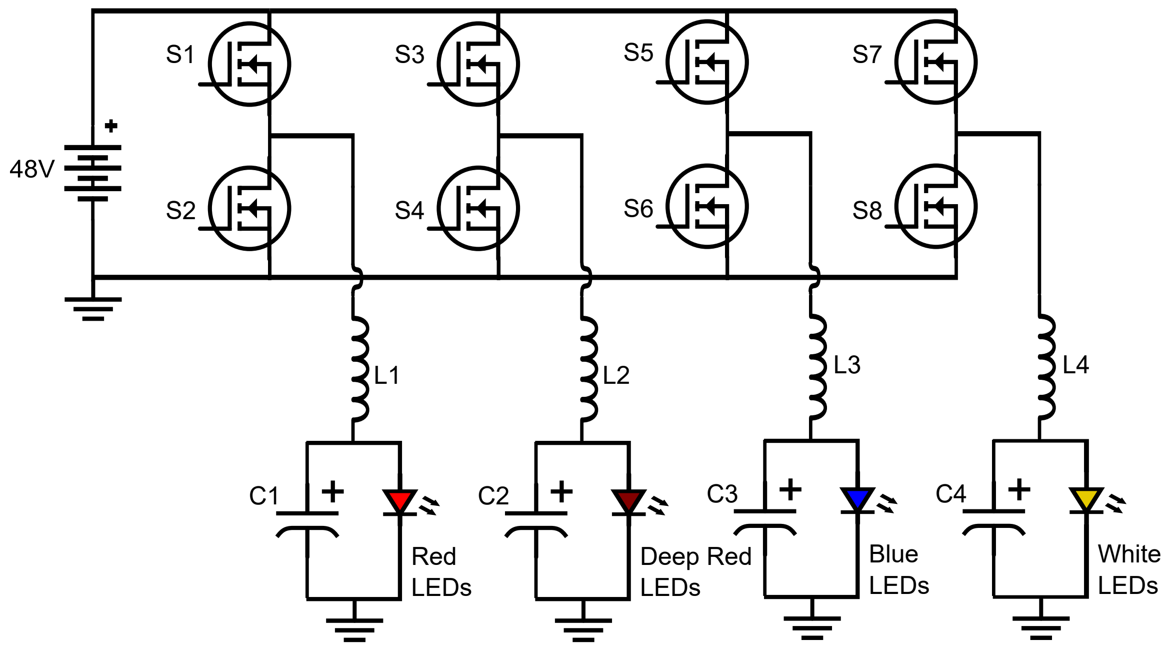

Figure 5.1: Synchronous Buck Based 4 Channel DC-DC Power Converter

(The N-Channel MOSFETs used come with an interal anti-parallel diode. Hence, it hasn't been explicitly shown in figure 5.1)
Following are some comments on the above DC-DC converter topology:

1. Complementary PWM switching of high-side and low-side switch of the power converter results in a controlled charging of the inductor which directly delivers the current to the LED load. Since the inductor gets charged only for a specific portion of total switching time, the output voltage is less than the input voltage which is a desirable characteristic in this case.

2. Unlike large electrolytic capacitors in other power converters, a small capacitor is put across the load to filter out the high frequency ripple in the current delivered by the inductor. This ensures that the LEDs draw current with very low ripple which not only improves their luminous efficacy but also prevents severe drop in LED life.

3. A large 0.25 W bleeder resistor is also placed across the load channel to drain out the excess current in case an LED in the array blows off due to any reason which would cause a rapid fluctuation in current drawn affecting the whole circuit.

5.4 Design of the Power Converter

5.4.1 Selection of Switching Device

Here, the DC source considered is 48 V and switching frequency is 50 kHz. Since the switching devices in this power converter are subjected to voltages under 200 V and the switching frequency is above 25-30 kHz, Silicon MOSFETs with very low drain-source resistance ($r_{DS}(ON)$) are the optimal choice for it.

5.4.2 Selection of Inductor and Output Filter Capacitor

Following figure shows the operation of synchronous buck converter with switching frequency f_{sw} and switching time period $T_{sw} = \frac{1}{f_{sw}}$.

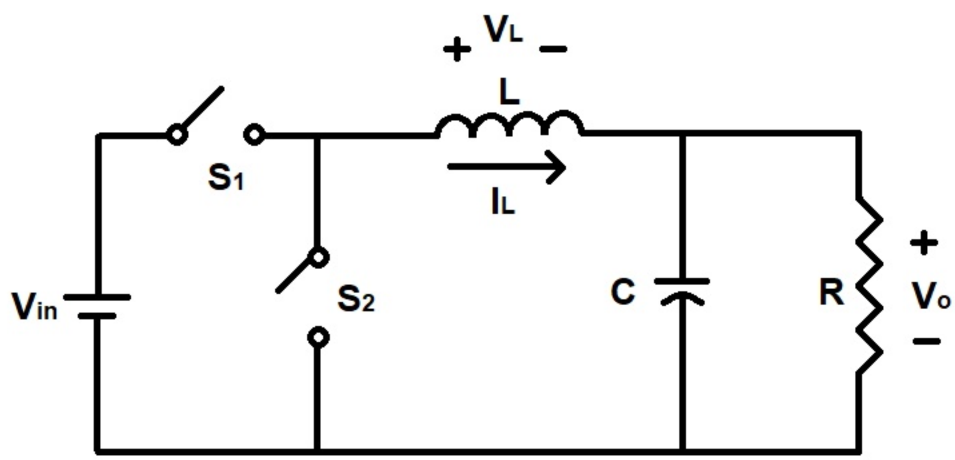

Figure 5.2: Synchronous Buck Converter Operation

Here, V_i is the input voltage, V_o is the output voltage. They are related by the equation:

$$V_o = D \times V_{in} \tag{5.1}$$

where D is the voltage tranformation ratio or duty ratio (between 0 and 1) for the PWM switching. V_L is the voltage across the inductor and I_L is the current flowing through the inductor. Switch S_1 is closed and S_2 is open for the ON time i.e $T_{ON} = DT_{sw}$. Switch S_2 is closed and S_1 is open for the OFF time i.e. $T_{OFF} = (1-D)T_{sw}$. Switches S_1 and S_2 are synchronously operated (with sufficient dead time $\approx \frac{T_{sw}}{4}$) to avoid short circuiting the DC power supply.

Selection of Inductor

The filter inductor value and its peak current are determined based on specified maximum inductor current ripple [10].
During the ON time, the inductor is subjected to voltage $V_L = V_i - V_o$. The relation between current and voltage for an inductor is given by the equation:

$$V_L = L \times \frac{dI_L}{dt} \tag{5.2}$$

where V_L is the voltage across the inductor, L is the inductance and I_L is the current flowing through the inductor. Here, inductor current itself is delivered to the load. Thus, output current $I_o = I_L$. If ΔI_L is the peak to peak ripple current for the inductor in ON time i.e. T_{ON}, from equation 5.2:

$$V_{in} - V_o = L\frac{\Delta I_L}{T_{ON}} = L\frac{\Delta I_L}{DT_{sw}} \tag{5.3}$$

Thus, if the maximum tolerable peak to peak ripple current ΔI_L is defined, the minimum value of inductance needed to maintain that can be calculated as:

$$L_{min} = \frac{(V_{in} - V_o)DT_{sw}}{\Delta I_L} \tag{5.4}$$

Here, input voltage is 48 V and the maximum peak to peak ripple current in each inductor of the topology has been restricted to 10% of the output current. As a thumb rule, 20% more inductance than the minimum required inductance is considered to accommodate current transients and non-idealities. Using this constraint and equation 5.4, inductances needed can be calculated easily. Following table summarizes the inductances needed for this topology:

Color of Light	V_o **(V)**	I_o **(A)**	D	L_{min} **(mH)**
Red	30.4	0.75	0.633	3.57
Deep Red	30	0.6	0.625	4.50
Blue	30.6	0.36	0.638	7.40
White	30.6	0.36	0.638	7.40

Table 5.2: Selection of Inductors

Selection of Output Filter Capacitor

Following diagram shows the inductor current I_L and capacitor current I_C for a synchronous buck converter:

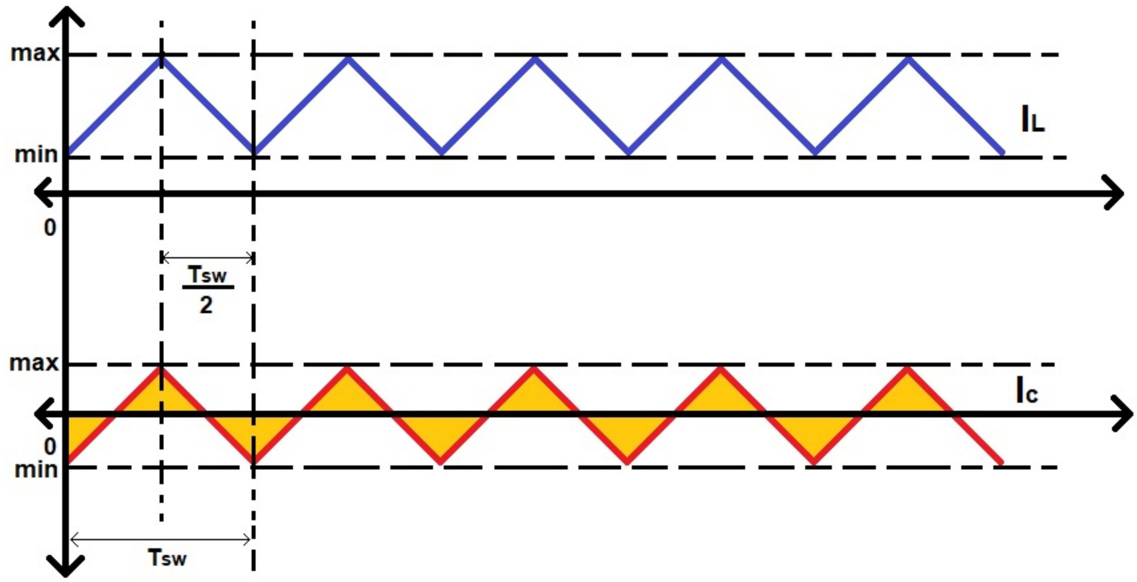

Figure 5.3: Currents in Synchronous Buck Converter

Peak to peak output voltage ripple (ΔV_o) is the main design criterion for the output filter capacitor. For ideal case i.e. zero output ripple voltage the steady state current flowing in the capacitor (I_C) should be zero [11]. Current voltage relation for capacitor is given by:

$$I_C = C \times \frac{dV_C}{dt} \tag{5.5}$$

where V_C is the voltage across the capacitor, C is the capacitance and I_C is the current flowing through the capacitor. Capacitor voltage itself is the output voltage of the buck converter i.e. $V_C = V_o$. The charge in capacitor due to ripple current is given by the area of the triangle shaded in yellow in figure 5.3 i.e. $Q_C = \frac{1}{2} I_C \Delta t = C \Delta V_C$. Here, the same ripple current from inductor flows in the capacitor. Thus, $\Delta I_C = \frac{\Delta I_L}{2}$.

The time for which this ripple current flows through the capacitor is $\Delta t = \frac{T_{ON} + TOFF}{2} = \frac{T_{sw}}{2}$. Substituting the above in expression for charge in the capacitor,

$$C\Delta V_o = C\Delta V_C = \Delta Q_C = \frac{1}{2} \times \frac{\Delta I_L}{2} \times \frac{T_{sw}}{2} \tag{5.6}$$

From equation 5.6, the minimum capacitance needed to keep the output voltage ripple in bounds is,

$$C_{min} = \frac{1}{8} \times \frac{\Delta I_L}{\Delta V_o f_{sw}} \tag{5.7}$$

Here, maximum peak to peak ripple voltage on each capacitor in the topology has been restricted to 10% of the output voltage. As a thumb rule, 20% more capacitance than the minimum required capacitance is considered to accommodate voltage transients and non-idealities. Using this constraint and equation 5.7, capacitances needed can be calculated easily. Following table summarizes the output filter capacitances needed for this topology:

Color of Light	V_o **(V)**	I_o **(A)**	D	C_{min} **(nF)**
Red	30.4	0.75	0.633	74.01
Deep Red	30	0.6	0.625	60
Blue	30.6	0.36	0.638	35.29
White	30.6	0.36	0.638	35.29

Table 5.3: Selection of Output Filter Capacitors

5.5 Control Strategy

Following figure shows the typical forward current (I_f) v/s forward voltage (V_f) characteristic for an LED:

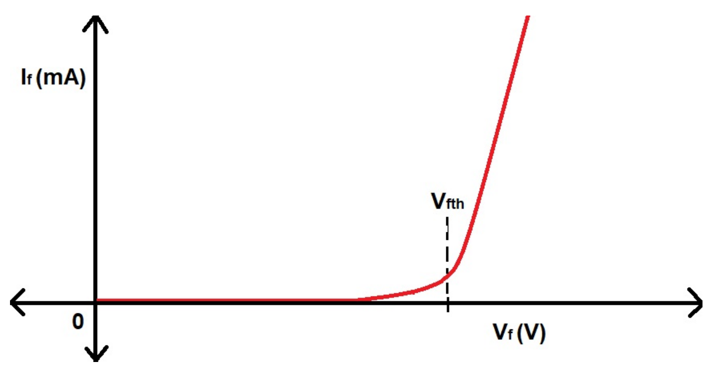

Figure 5.4: I-V Characteristics of an LED

Since the LEDs are non-ohmic, their forward I-V characteristics are such that a small change in voltage in above the threshold V_f causes a large change in current flowing through them. With a current mode control, any changes in current above the rated forward current don't result into large voltage fluctuations. The voltage across LEDs remains nearly constant for any current above the knee point.

Current mode control for a buck converter is simple to design and optimize. Hence current mode control has been preferably chosen over voltage mode control here.

5.6 Design of the Current Control System

Current flowing through the inductor in a buck converter is directly governed by the PWM duty ratio D. Since the current flowing through the inductor needs to be controlled in order to control the PPFD generated by the LEDs, a transfer function from duty ratio to inductor current has to be derived. This transfer function will serve as the plant in the control system.

5.6.1 Small Signal Analysis of Synchronous Buck Converter in CCM

In order to derive a transfer function from fractional change in PWM duty ratio D to inductor current I_L for CCM, the operation of synchronous buck converter in its two states viz. ON and OFF has to be studied.

It is very beneficial to obtain non-switching average models of these switch-mode converters for simulating the converter performance under dynamic conditions caused by the change of input voltage and/or the output load. Under the dynamic condition, the converter duty-ratio, and the average values of voltages and currents within the converter vary with time, but relatively slowly, with frequencies in an order of magnitude smaller than the switching frequency [12].

Note: Here a slightly different notation has been used. All lower case letters with caps indicate fractionally small increments in quantities and all upper case letters indicate DC quantities.

Here, V_{in} is input voltage, V_o is output voltage, I_o is output current, I_L is inductor current and I_C is capacitor current. L, C and R represent inductor, output filter capacitor and load resistor respectively.

Small signal analysis of buck converter involves adding an infinitely small perturbation to all the terms in the differential equations relating voltage and current with duty ratio [13]. Thus, the final transfer function obtained will be a transfer function from perturbation in duty ratio to the resulting perturbation in inductor current which is, $G(s) = \frac{\hat{i_L(s)}}{\hat{d(s)}}$.

Operation in ON State

Following figure shows the ON state operation of a CCM synchronous buck converter:

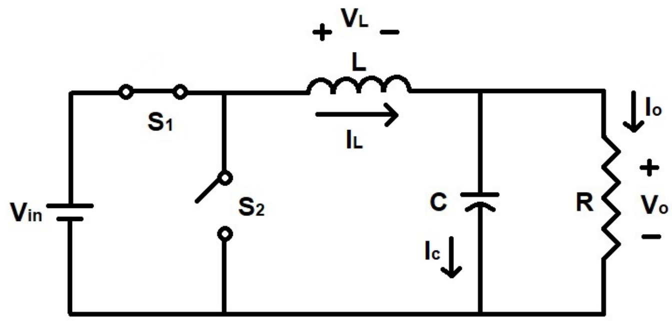

Figure 5.5: Synchronous Buck Converter in ON State

In ON state of the synchronous buck converter, switch S_1 is closed and switch S_2 is open. The voltage across inductor is $V_L = V_{in} - V_o = L \times \frac{dI_L}{dt}$. Thus,

$$\frac{dI_L(t)}{dt} = \frac{dV_{in}(t)}{L} - \frac{dV_o(t)}{L} \tag{5.8}$$

From figure 5.5, $I_L(t) = I_C(t) + I_o(t)$. Thus,

$$I_L(t) = C\frac{dV_C(t)}{dt} + \frac{V_C(t)}{R} \tag{5.9}$$

From above,

$$\frac{dV_C(t)}{dt} = \frac{1}{C}I_L(t) - \frac{V_C(t)}{RC} \tag{5.10}$$

Here, output voltage itself is capacitor voltage. Thus, $V_o(t) = V_C(t)$.

Consider state vector $x = \begin{bmatrix} I_L(t) \\ V_C(t) \end{bmatrix}$, input vector $u = V_{in}(t)$ and

output vector $y = I_o(t) = \frac{V_C(t)}{R}$ for the state-space representation of the above system in form $\dot{x} = A_1 x + B_1 u$ and $y = C_1 x + D_1 u$.

Thus state-space representation of the above system is,
$\dot{x} = \begin{bmatrix} 0 & \frac{-1}{L} \\ \frac{1}{C} & \frac{-1}{RC} \end{bmatrix} x + \begin{bmatrix} \frac{1}{L} \\ 0 \end{bmatrix} u$ and $y = \begin{bmatrix} 0 & \frac{1}{R} \end{bmatrix} x + 0u$.

Operation in OFF State

Following figure shows the OFF state operation of a CCM synchronous buck converter:

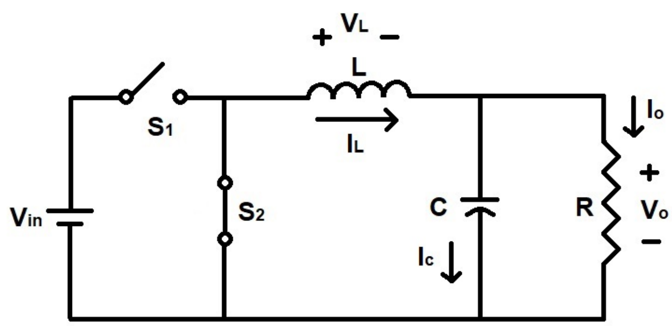

Figure 5.6: Synchronous Buck Converter in OFF State

In OFF state of the synchronous buck converter, switch S_2 is closed and switch S_1 is open. The voltage across inductor is $V_L = -V_o = L \times \frac{dI_L}{dt}$. Thus,

$$\frac{dI_L(t)}{dt} = -\frac{dV_C(t)}{L} \tag{5.11}$$

From figure 5.6, $I_C(t) = I_L(t) - I_o(t)$. Thus,

$$C\frac{dV_C(t)}{dt} = I_L(t) - \frac{V_C(t)}{R} \tag{5.12}$$

From above,

$$\frac{dV_C(t)}{dt} = \frac{1}{C}I_L(t) - \frac{V_C(t)}{RC} \tag{5.13}$$

Here, output voltage itself is capacitor voltage. Thus, $V_o(t) = V_C(t)$.

Consider state vector $x = \begin{bmatrix} I_L(t) \\ V_C(t) \end{bmatrix}$, input vector $u = V_{in}(t)$ and

output vector $y = I_o(t) = \frac{V_C(t)}{R}$ for the state-space representation of the above system in form $\dot{x} = A_2x + B_2u$ and $y = C_2x + D_2u$.

Thus state-space representation of the above system is,
$\dot{x} = \begin{bmatrix} 0 & \frac{-1}{L} \\ \frac{1}{C} & \frac{-1}{RC} \end{bmatrix} x + \begin{bmatrix} 0 \\ 0 \end{bmatrix} u$ and $y = \begin{bmatrix} 0 & \frac{1}{R} \end{bmatrix} x + 0u$.

In order to establish an average state space model $\dot{x} = Ax + Bu$ and $y = Cx + Du$ for the CCM synchronous buck converter, we need to compute the time averaged matrices A, B, C and D which can be done as follows:
In ON state, the time for which switch S_1 is closed is DT_{sw} and in OFF state the time for which switch S_2 is closed is $(1-D)T_{sw}$. From above, the time averaged matrices are,

- $A_{avg} = DA_1 + (1-D)A_2 = \begin{bmatrix} 0 & \frac{-1}{L} \\ \frac{1}{C} & \frac{-1}{RC} \end{bmatrix}$
- $B_{avg} = DB_1 + (1-D)B_2 = \begin{bmatrix} \frac{D}{L} \\ 0 \end{bmatrix}$
- $C_{avg} = DC_1 + (1-D)C_2 = \begin{bmatrix} 0 & \frac{1}{R} \end{bmatrix}$
- $D_{avg} = DD_1 + (1-D)D_2 = 0$

Hence, the system can be represented now as, $\dot{x} = A_{avg}x + B_{avg}u$ and $y = C_{avg}x + D_{avg}u$.

Now, consider that fractionally small increments are done in all the quantities associated with vectors x, u and y to slightly perturb them. This means the following:

- $I_L(t) = I_L(t) + \hat{i_L}(t)$
- $V_C(t) = V_C(t) + \hat{v_C}(t)$
- $D(t) = D(t) + \hat{d}(t)$
- $V_{in}(t) = V_{in}(t) + \hat{v_{in}}(t)$
- $I_o(t) = I_o(t) + \hat{i_o}(t)$

From above, the final state space representation of the system is:

$$\begin{bmatrix} \frac{d(I_L(t)+\hat{i_L}(t))}{dt} \\ \frac{d(V_C(t)+\hat{v_C}(t))}{dt} \end{bmatrix} = \begin{bmatrix} 0 & \frac{-1}{L} \\ \frac{1}{C} & \frac{-1}{RC} \end{bmatrix} \begin{bmatrix} I_L(t) + \hat{i_L}(t) \\ V_C(t) + \hat{v_C}(t) \end{bmatrix} + \begin{bmatrix} \frac{D(t)+\hat{d}(t)}{L} \\ 0 \end{bmatrix} (V_{in}(t) + \hat{v_{in}}(t)) \tag{5.14}$$

and

$$(I_o(t) + \hat{i_o}(t)) = \begin{bmatrix} 0 & \frac{1}{R} \end{bmatrix} \begin{bmatrix} I_L(t) + \hat{i_L}(t) \\ V_C(t) + \hat{v_C}(t) \end{bmatrix} + 0(V_{in}(t) + \hat{v_{in}}(t)) \tag{5.15}$$

From the above state space representation, DC and small signal analysis can be performed as follows:

1. **DC Analysis**

   In DC or steady state there is no perturbation in quantities and the average change in inductor current and capacitor voltage is zero. Thus, the state space equation becomes $0 = A_{avg}x + B_{avg}u$. Hence, $x = -A_{avg}^{-1}Bu$.

   $$\begin{bmatrix} I_L \\ V_C \end{bmatrix} = -\begin{bmatrix} \frac{-L}{R} & C \\ -L & 0 \end{bmatrix} V_{in}.$$

   This gives, $I_L = \frac{DV_{in}}{R}$ and $V_C = V_o = DV_{in}$ verifying the initial definition of voltage transformation ratio.

2. **Small Signal Analysis**

   Considering all the DC quantities have been removed, we are left only with the perturbations. Neglecting product of incremental quantities in equation 5.14 and 5.15, the state space equations become:

   $$\begin{bmatrix} \frac{d\hat{i_L(t)}}{dt} \\ \frac{d\hat{v_C(t)}}{dt} \end{bmatrix} = \begin{bmatrix} 0 & \frac{-1}{L} \\ \frac{1}{C} & \frac{-1}{RC} \end{bmatrix} \begin{bmatrix} \hat{i_L(t)} \\ \hat{v_C(t)} \end{bmatrix} + \begin{bmatrix} \frac{D(t)}{L} \\ 0 \end{bmatrix} \hat{v_{in}(t)} + \begin{bmatrix} \frac{\hat{d(t)}}{L} \\ 0 \end{bmatrix} V_{in}(t) \tag{5.16}$$

   $$\hat{i_o(t)} = \begin{bmatrix} 0 & \frac{1}{R} \end{bmatrix} \begin{bmatrix} \hat{i_L(t)} \\ \hat{v_C(t)} \end{bmatrix} \tag{5.17}$$

5.6.2 Plant Transfer Function

The plant transfer function for this control system is the one from perturbation in duty ratio to the resulting perturbation in inductor current. It can be derived from equation 5.16 by taking its Laplace transform as follows:

$s\hat{i_L(s)} = \frac{-V_C(s)}{L} + \frac{D\hat{v_{in}(s)}}{L} + \hat{d(s)}\frac{V_{in}}{L}$. Considering no perturbation in input,

$$s\hat{i_L(s)} = \frac{-V_C(s)}{L} + \hat{d(s)}\frac{V_{in}}{L} \tag{5.18}$$

. $s\hat{v_C(s)} = \frac{\hat{i_L(s)}}{C} - \frac{\hat{v_C(s)}}{RC}$. Thus,

$$\hat{v_C(s)} = \frac{R}{RCs+1}\hat{i_L(s)} \tag{5.19}$$

Substituting $\hat{v_C(s)}$ from equation 5.19 into equation 5.18, $s\hat{i_L(s)} = -\frac{R}{L(RCs+1)}\hat{i_L(s)} + \hat{d(s)}\frac{V_{in}}{L}$.

From above, $\left[s+\frac{R}{L(RCs+1)}\right]\hat{i_L(s)} = \hat{d(s)}\frac{V_{in}}{L}$. Thus,

$$\frac{\hat{i_L(s)}}{\hat{d(s)}} = \frac{V_{in}(RCs+1)}{RLCs^2+Ls+R} \tag{5.20}$$

Thus, the plant transfer function for this control system is, $G(s) = \frac{\hat{i_L(s)}}{\hat{d(s)}} = \frac{V_{in}(RCs+1)}{RLCs^2+Ls+R}$.
Note: Since LEDs have dynamic resistance beyond the knee point on the I-V characteristic, they have been represented by constant resistance calculated by linearizing the I-V curve at the operating point.

Parameters for Colors of Light

For all the 4 converter channels corresponding to different colors of light discussed here, the values of R can be calculated as effective resistance. Values of R, L and C can be summarized in the following table:

Color of Light	R(Ω)	L(mH)	C(nF)
Red	40.53	3.57	74.01
Deep Red	50	4.5	60
Blue	85	7.4	35.29
White	85	7.4	35.29

Table 5.4: R,L,C for 4 Converter Channels

Frequency and step response of G(s)

Substituting values of R, L and C from table 5.4 into equation 5.20, the transfer function $G(s)$ can be calculated for all 4 channels.
Note: For the controller design, subscripts r, d, b and w indicate transfer functions for Channel 1: Red, Channel 2: Deep Red, Channel 3: Blue and Channel 4: White.

Following are the frequency responses and step responses of $G(s)$ generated using *MATLAB* for all 4 channels of the converter which are:

1. $G_r(s)$
2. $G_d(s)$
3. $G_b(s)$
4. $G_w(s)$

1. **Channel 1: Red** - $G_r(s) = \frac{1.44\times10^{-4}s+48}{1.071\times10^{-8}s^2+3.57\times10^{-3}s+40.53}$

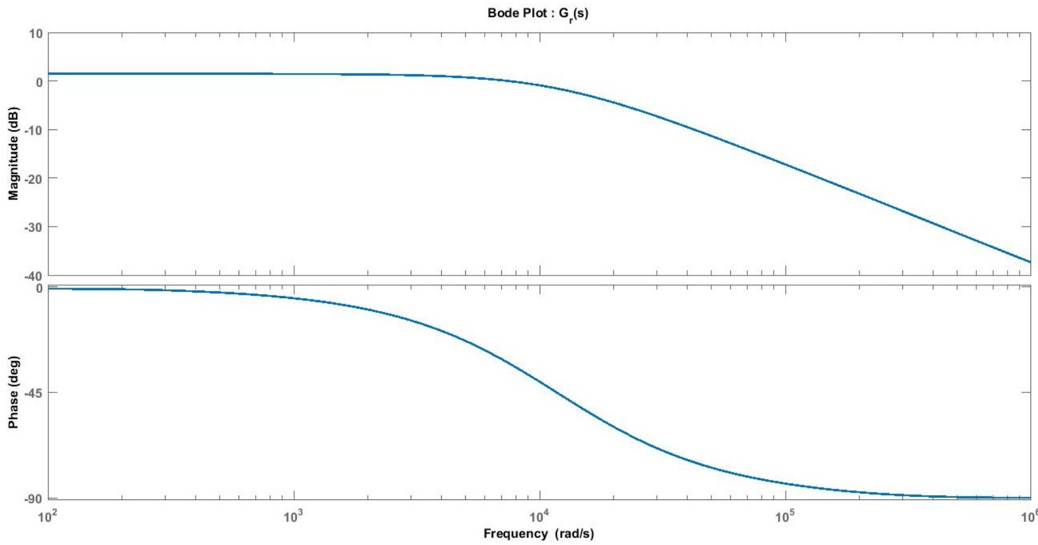

Figure 5.7: Bode Plot for $G_r(s)$

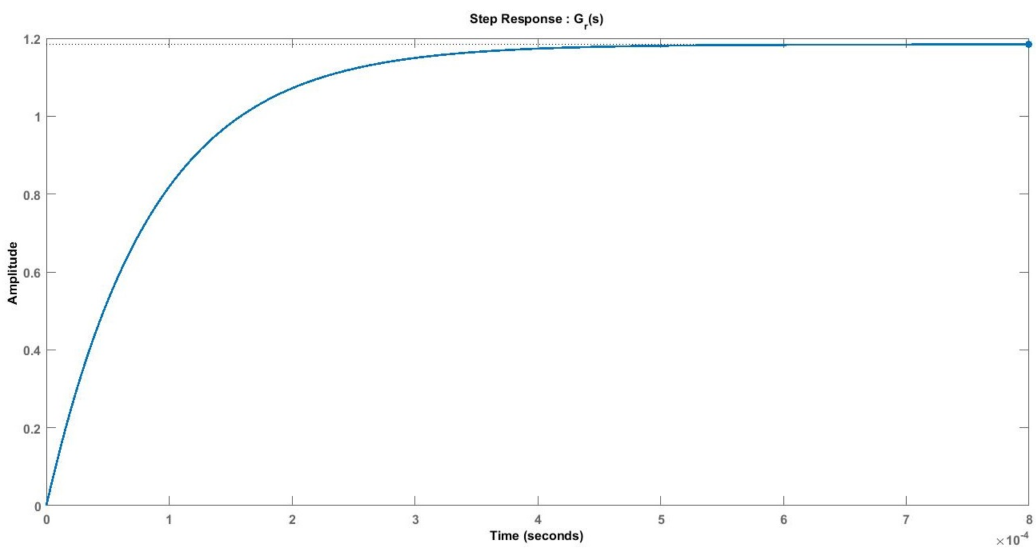

Figure 5.8: Step Response for $G_r(s)$

2. **Channel 2: Deep Red** - $G_d(s) = \frac{1.44\times10^{-4}s+48}{1.35\times10^{-8}s^2+4.5\times10^{-3}s+50}$

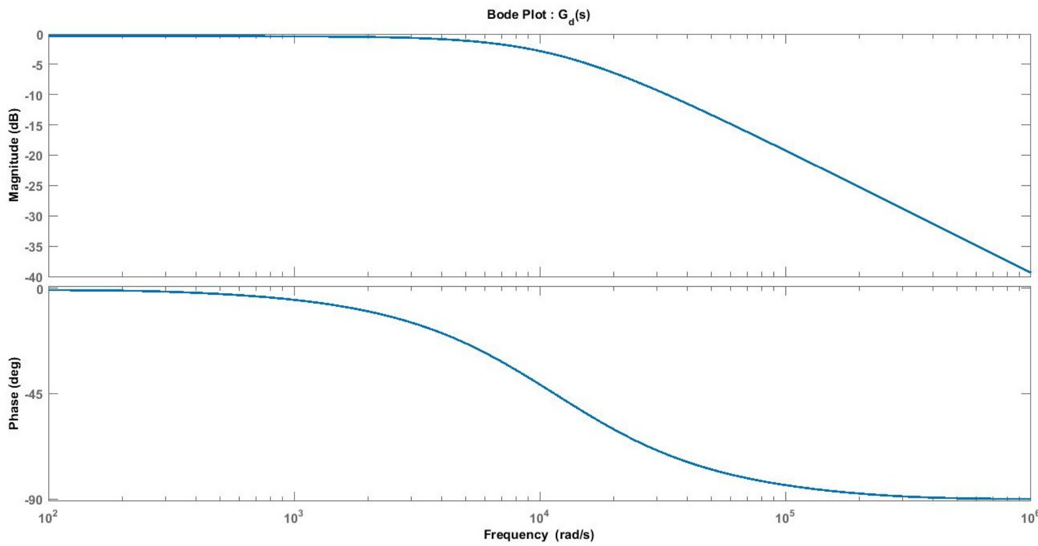

Figure 5.9: Bode Plot for $G_d(s)$

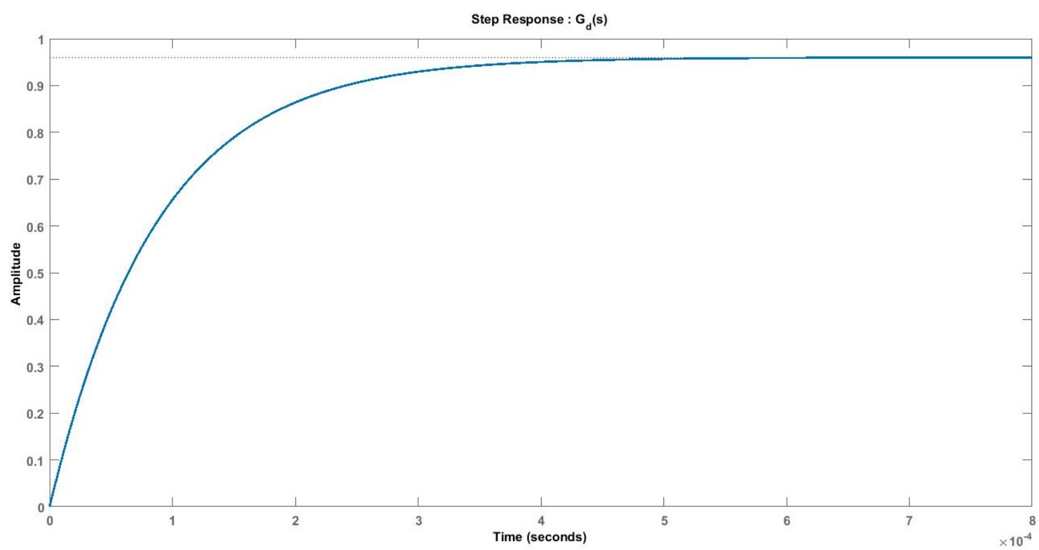

Figure 5.10: Step Response for $G_d(s)$

3. **Channel 3: Blue** - $G_b(s) = \frac{1.44\times10^{-4}s+48}{2.22\times10^{-8}s^2+7.4\times10^{-3}s+85}$

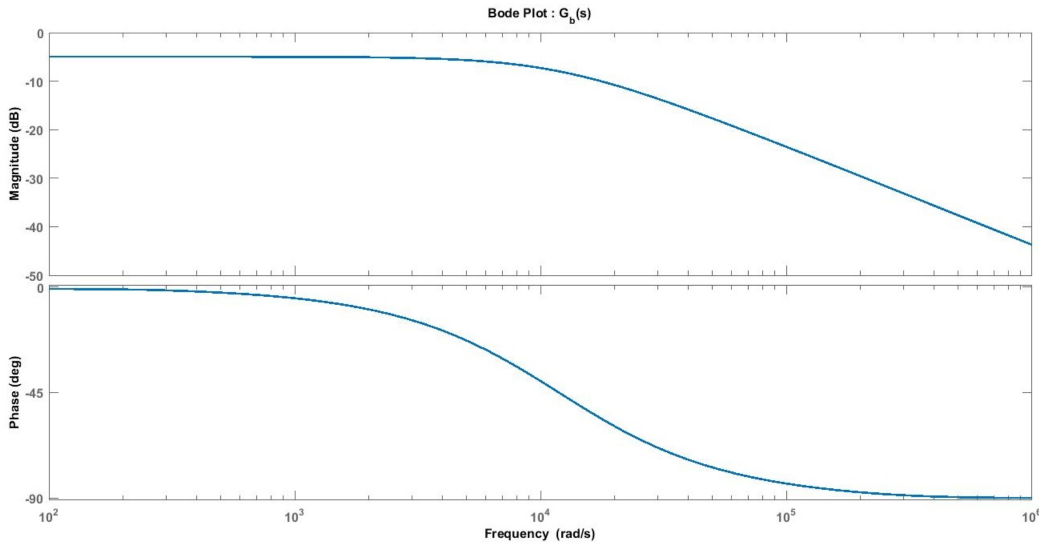

Figure 5.11: Bode Plot for $G_b(s)$

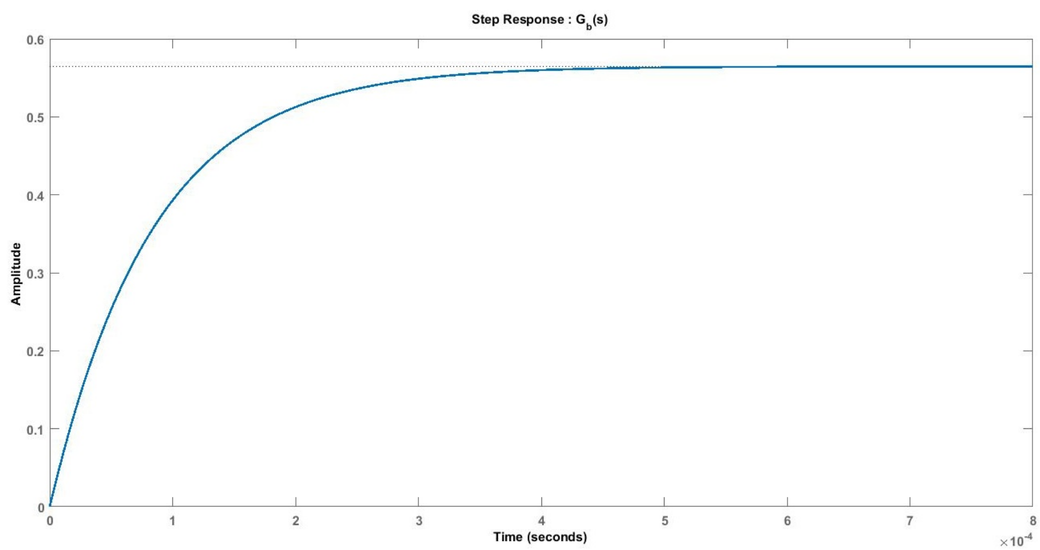

Figure 5.12: Step Response for $G_b(s)$

4. **Channel 4: White** - $G_w(s) = \frac{1.44\times10^{-4}s+48}{2.22\times10^{-8}s^2+7.4\times10^{-3}s+85}$

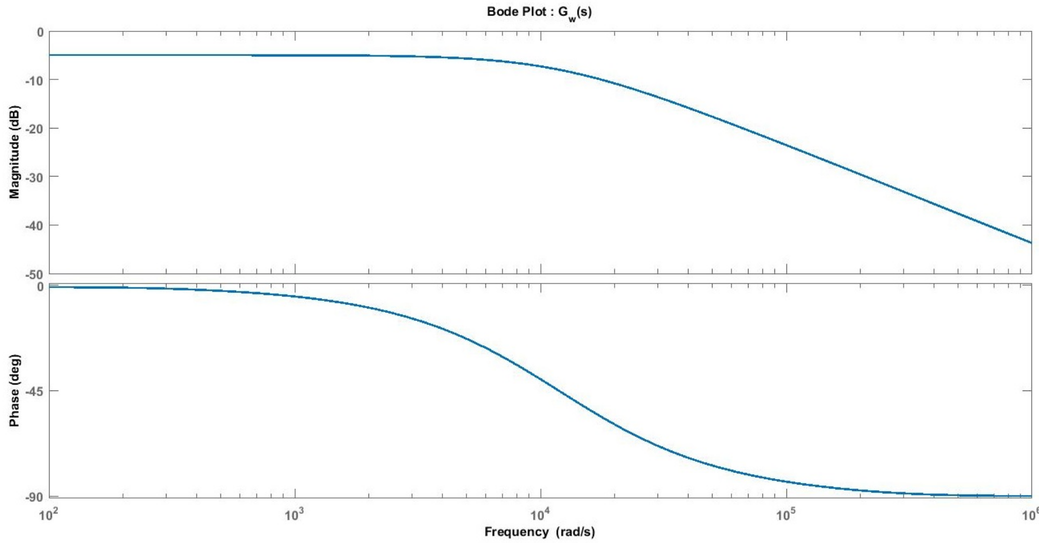

Figure 5.13: Bode Plot for $G_w(s)$

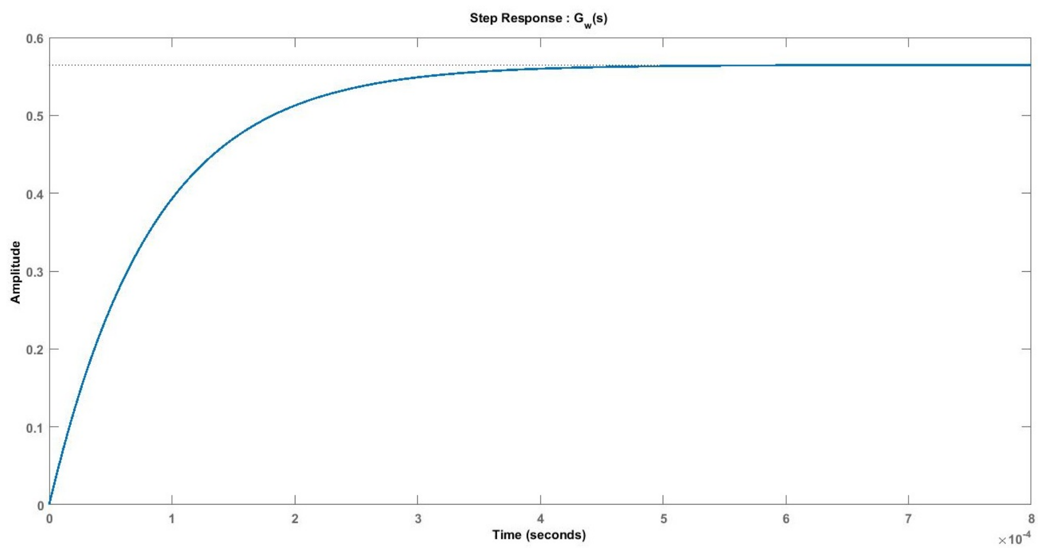

Figure 5.14: Step Response for $G_w(s)$

5.6.3 Selection of and Design of Controller

Choice of Controller

The plant in this control system is a second order transfer function with bode plots as mentioned above. Since the Grow-light system imitates the sunlight, the reference inputs for the control system are not going to change dynamically. Here, an accurate tracking of the reference inputs is expected but the transient response does not have to be extremely fast like the controllers in dynamic current control systems.
Following are the constraints for the controller design:

1. Closed loop stability of the system
2. Zero steady state error in reference tracking
3. Fairly fast transient response for tracking step changes in reference input

To satisfy all the above conditions, a proportional-integral (PI) controller is the best choice which is easy to implement and achieves satisfactory results. The PI controller considered here is of parallel form i.e. $K(s) = k_p + \frac{k_i}{s}$ where k_p is proportional gain and k_i is integral gain. For satisfying all the above conditions, following constraints are placed on the PI controller design:

1. Open Loop Gain Margin $\geq 6dB$
2. Open Loop Phase Margin $\geq 60°$

Design of PI Controller

Following is a diagram of closed loop control system designed here:

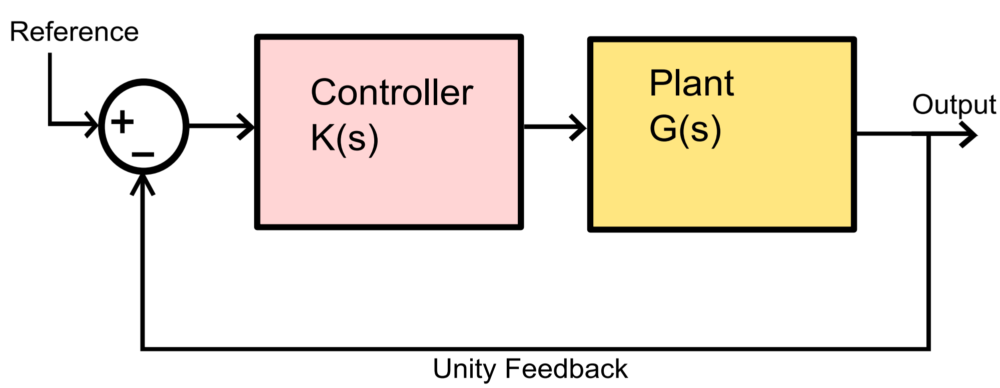

Figure 5.15: Closed Loop Control System

The error signal which is difference between reference signal and output of the plant is fed to the controller which generates controlled input in order to match the plant output with the reference provided.
Here, plant transfer function is $G(s) = \frac{V_{in}(RCs+1)}{RLCs^2+Ls+R}$ and compensator transfer function is $K(s) = k_p + \frac{k_i}{s}$. Following are the design constraints for the system:

- Gain Crossover Frequency ω_c = $\frac{1}{100} \times f_{sw}$ = $\frac{2\pi}{100} \times 50000$ = 3140 rad/s as required for successful hardware implementation

- Open Loop Phase Margin = 80°

Substituting $s = j\omega$ in equations for $G(s)$ and $K(s)$:

- $G(j\omega) = \frac{V_{in}(jRC\omega+1)}{-RLC\omega^2+jL\omega+R}$

- $K(j\omega) = k_p - \frac{k_i}{\omega}$

From above, loop transfer function is $L(j\omega) = G(j\omega) \times K(j\omega) = \frac{V_{in}(1+j\omega RC)(k_p - j\frac{k_i}{\omega})}{(R-RLC\omega^2)+jL\omega}$.

Now, at $\omega = \omega_c$, $|L(j\omega)| = 1$. Thus,

$$\frac{V_{in}\sqrt{1+\omega_c^2R^2C^2}\sqrt{k_p^2+\frac{k_i^2}{\omega_c^2}}}{\sqrt{(R-RLC\omega_c^2)^2+L^2\omega_c^2}} = 1 \tag{5.21}$$

Also, Open Loop Phase Margin = 180° + $\angle L(j\omega_c)$. Thus,

$$tan^{-1}(\omega_c RC) - tan^{-1}\left(\frac{k_i}{\omega_c k_p}\right) - tan^{-1}\left(\frac{L\omega_c}{R-RLC\omega_c^2}\right) + 180^\circ = 80^\circ \tag{5.22}$$

Let $\alpha = \frac{k_i}{k_p}$. This ratio of gains has to satisfy both the above equations. From equation 5.22,

$$\alpha = -\omega_c \times \left[80^\circ - 180^\circ + tan^{-1}\left(\frac{L\omega_c}{R-RLC\omega_c^2}\right) - tan^{-1}(\omega_c RC)\right] \tag{5.23}$$

Substituting $k_i = \alpha k_p$ in equation 5.21,

$$k_p = \frac{\sqrt{R-RLC\omega_c^2+L^2\omega_c^2}}{V_{in}\sqrt{1+\omega_c^2R^2C^2}\sqrt{1+\frac{\alpha^2}{\omega_c^2}}} \tag{5.24}$$

Now, k_i can be easily calculated as $k_i = \alpha k_p$.

Using the above procedure of first calculating the ratio of integral gain to proportional gain and then to calculate the individual gains in order to satisfy the ω_c and open loop phase margin requirements, the controller gains have been calculated for all 4 channels of the power converter as follows:

Channel	**Color of Light**	k_p	k_i
1	Red	0.0756	2.735×10^3
2	Deep Red	0.0995	3.377×10^3
3	Blue	0.1531	5.733×10^3
4	White	0.1531	5.733×10^3

Table 5.5: PI Controller Gains for 4 Channels

Using these controller gains, following controller transfer functions can be defined:

1. $K_r(s) = 0.0756 + \frac{2.735\times10^3}{s}$
2. $K_d(s) = 0.0995 + \frac{3.377\times10^3}{s}$
3. $K_b(s) = 0.1531 + \frac{5.733\times10^3}{s}$
4. $K_w(s) = 0.1531 + \frac{5.733\times10^3}{s}$

For the closed loop control system, the closed loop transfer function $T(s)$ can be calculated as $T(s) = \frac{G(s)K(s)}{1+G(s)K(s)} = \frac{L(s)}{1+L(s)}$.
For all the 4 channels, the summary of transfer functions is as follows:

Channel	**Plant**	**Controller**	**Open Loop**	**Closed Loop**
1:Red	$G_r(s)$	$K_r(s)$	$L_r(s) = G_r(s)K_r(s)$	$T_r(s) = \frac{L_r(s)}{1+L_r(s)}$
2:Deep Red	$G_d(s)$	$K_d(s)$	$L_d(s) = G_d(s)K_d(s)$	$T_d(s) = \frac{L_d(s)}{1+L_d(s)}$
3:Blue	$G_b(s)$	$K_b(s)$	$L_b(s) = G_b(s)K_b(s)$	$T_b(s) = \frac{L_b(s)}{1+L_b(s)}$
4:White	$G_w(s)$	$K_w(s)$	$L_w(s) = G_w(s)K_w(s)$	$T_w(s) = \frac{L_w(s)}{1+L_w(s)}$

Table 5.6: Caption

5.6.4 Closed Loop Response

Following are the frequency responses and step responses of $T(s)$ generated using *MATLAB* for all 4 channels of the converter:

1. **Channel 1: Red** -

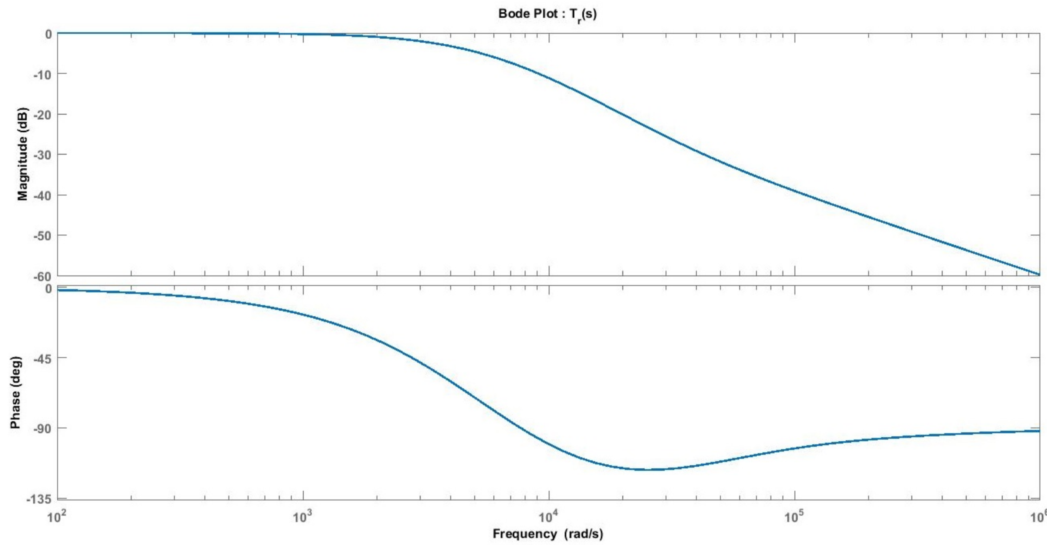

Figure 5.16: Bode Plot for $T_r(s)$

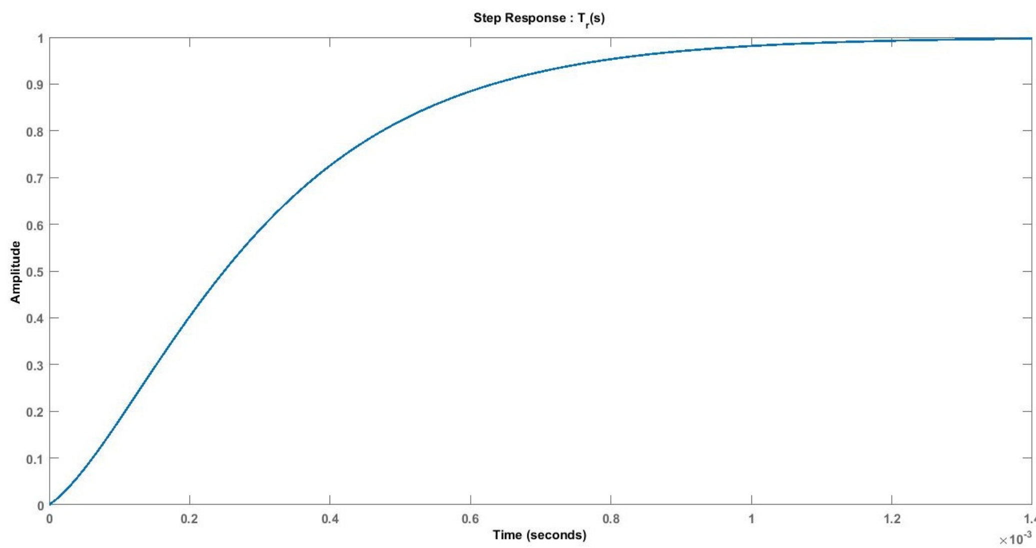

Figure 5.17: Step Response for $T_r(s)$

2. **Channel 2: Deep Red -**

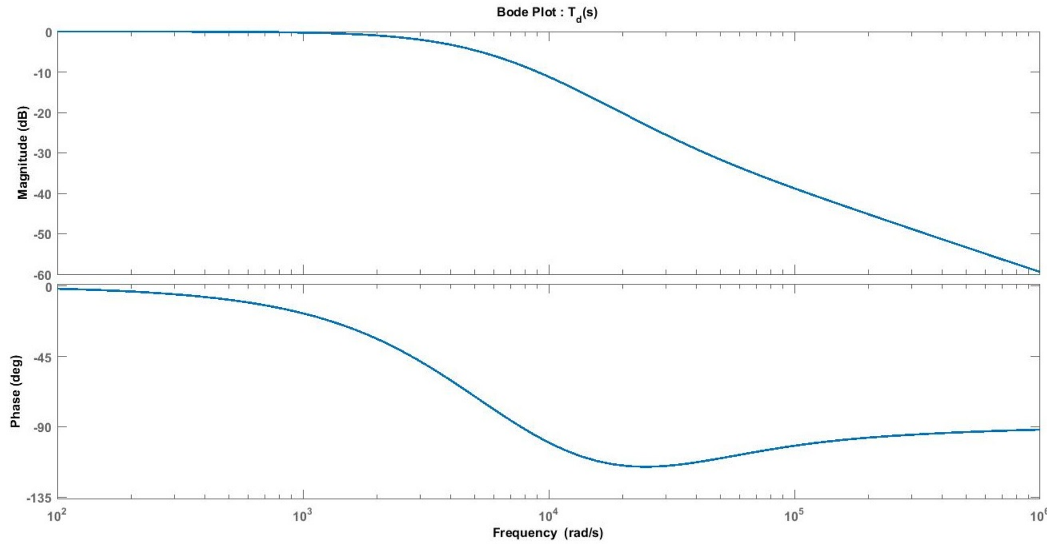

Figure 5.18: Bode Plot for $T_d(s)$

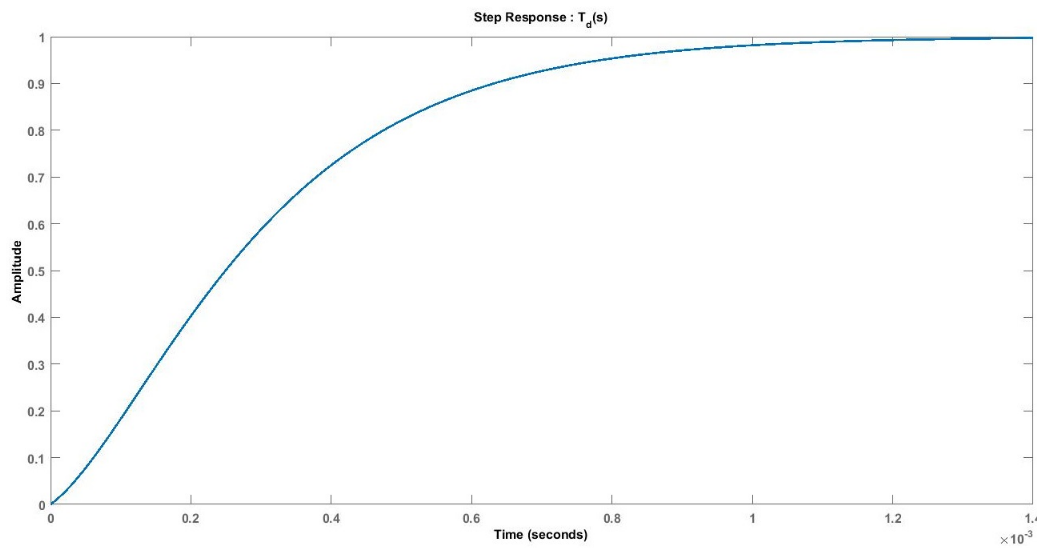

Figure 5.19: Step Response for $T_d(s)$

3. **Channel 3: Blue** -

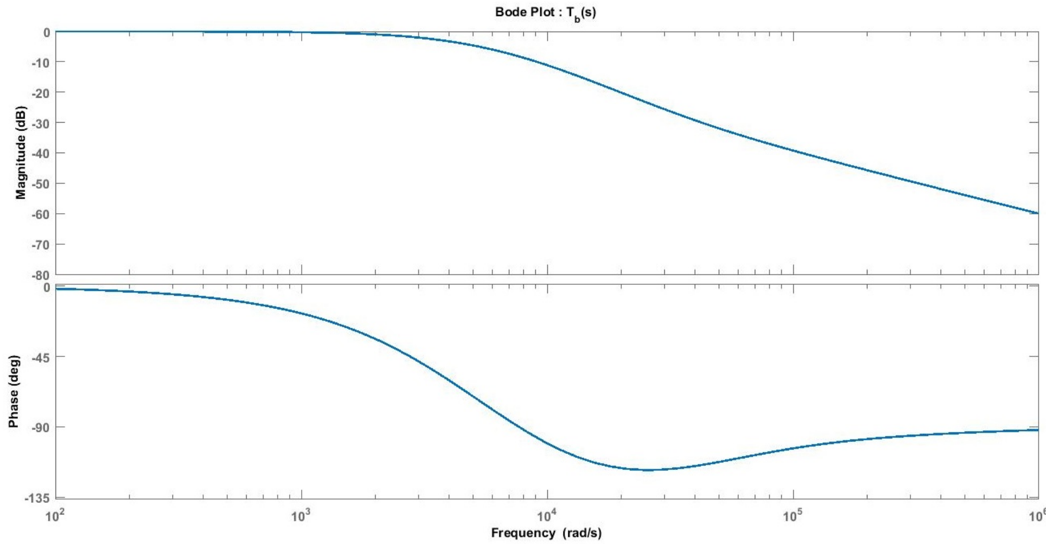

Figure 5.20: Bode Plot for $T_b(s)$

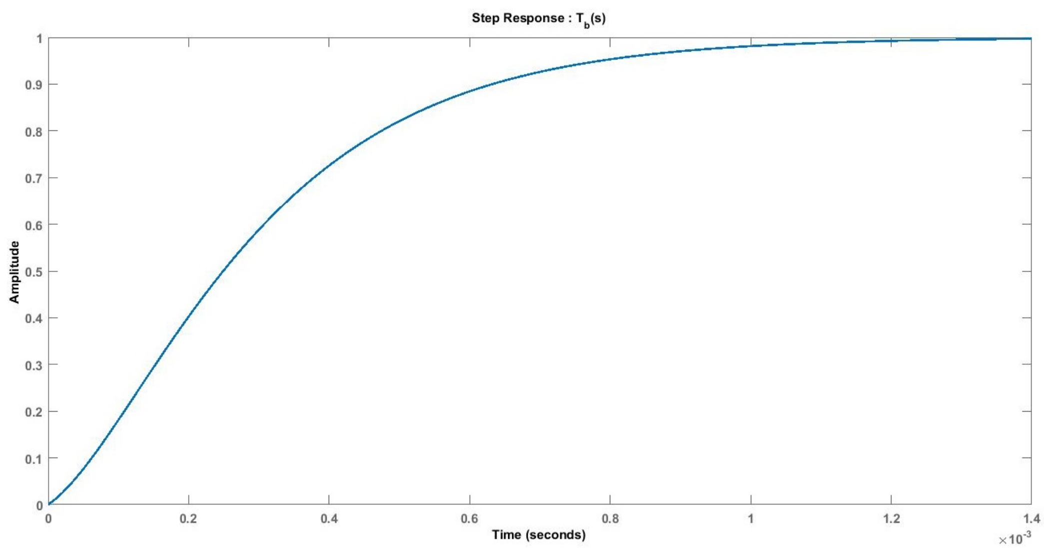

Figure 5.21: Step Response for $T_b(s)$

4. **Channel 4: White** -

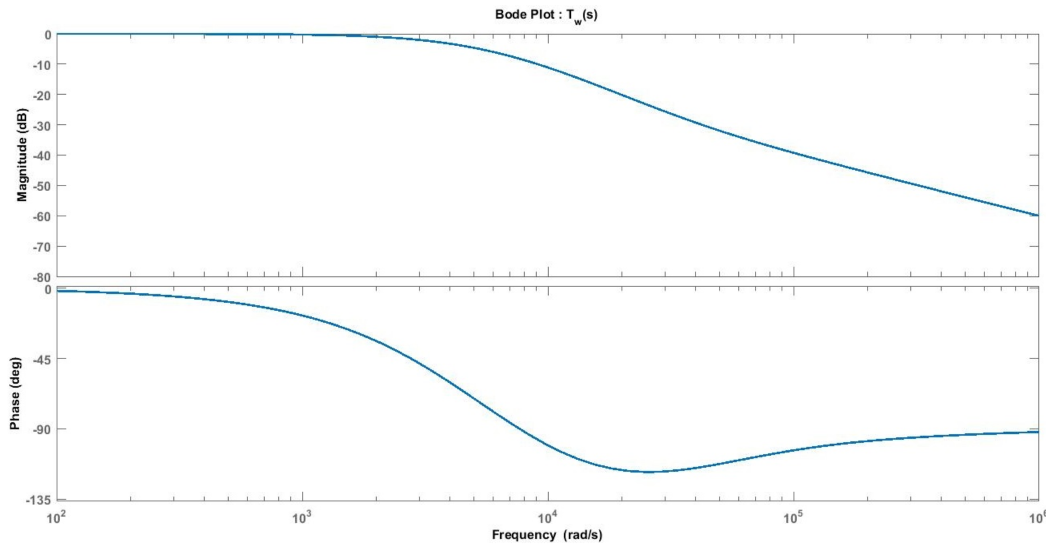

Figure 5.22: Bode Plot for $T_w(s)$

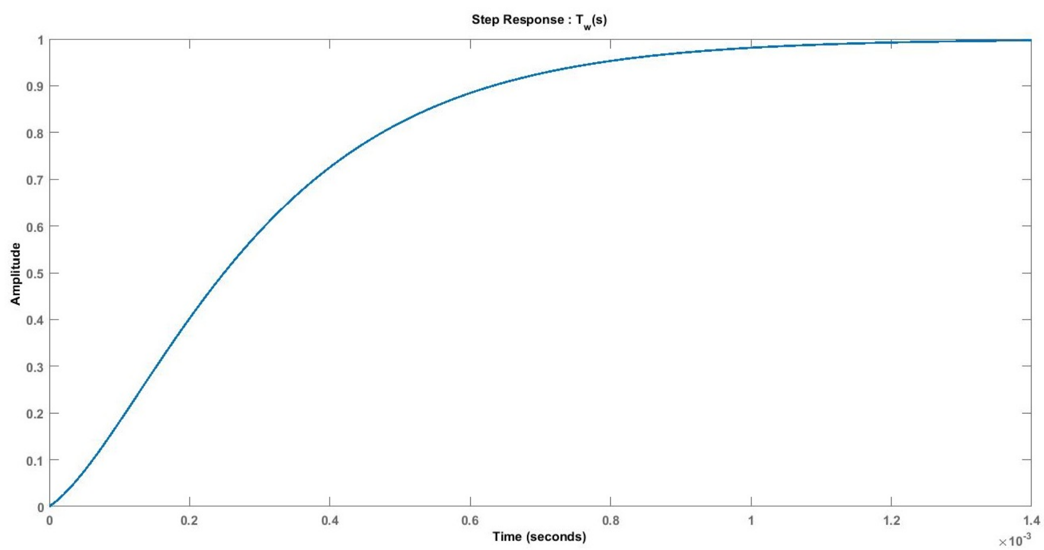

Figure 5.23: Step Response for $T_w(s)$

Chapter 6

Simulation Studies

The LED Grow-light system has been modelled and simulated using *MATLAB Simulink*.

6.1 Current Reference Settings

3 modes have been designed for operation of the Grow-light system which are as follows:

1. VG (Vegetative Growth) Mode
2. FB (Flowering Boost) Mode
3. AL (Aesthetic Lighting) Mode

The reference currents corresponding to these modes for 4 channels are viz. I_r^*, I_d^*, I_b^* and I_w^* respectively for Red, Deep Red, Blue and White light. Following is the description of reference inputs to the control system based on these 3 modes:

Mode	**Description**	I_r^* (A)	I_d^* (A)	I_b^* (A)	I_w^* (A)
VG	Promotes vegetative growth (R/FR=2)	0.75	0.3	0.36	0.18
FB	Promotes flowering (R/FR=0.5)	0.35	0.6	0.18	0.18
AL	Keeps only White LEDs ON	0	0	0	0.36

Table 6.1: LED Growlights: Modes of Operation

Following figure shows the reference currents given to the control system for simulation in *MATLAB Simulink*:

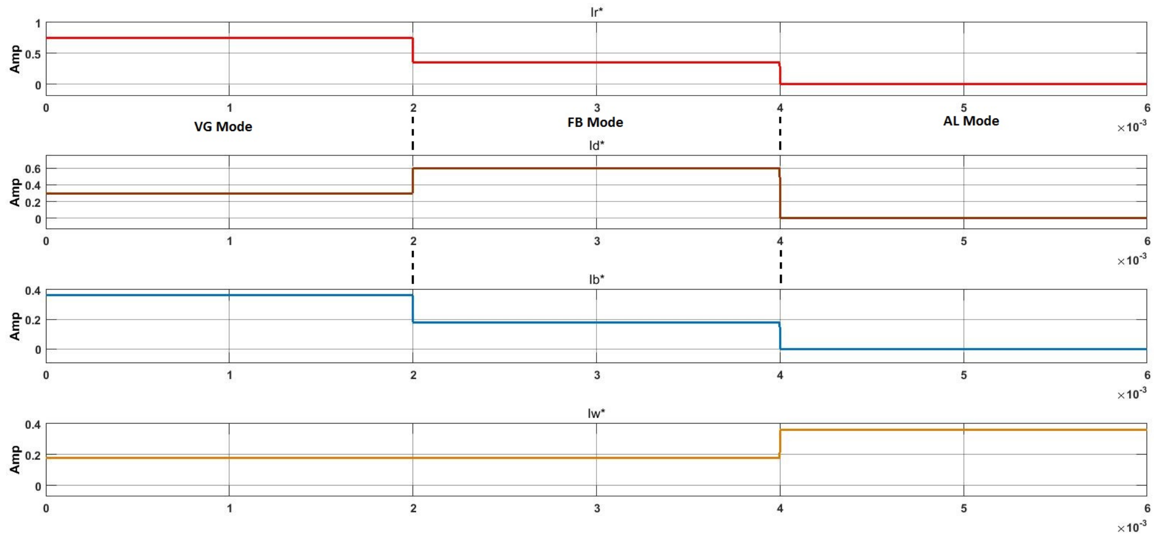

Figure 6.1: Current References for 3 Modes of Lighting

6.2 System Model

Following shows the *MATLAB Simulink* model of the LED Grow-light system with DC power source, DC-DC converter, LED arrays and the current controller:

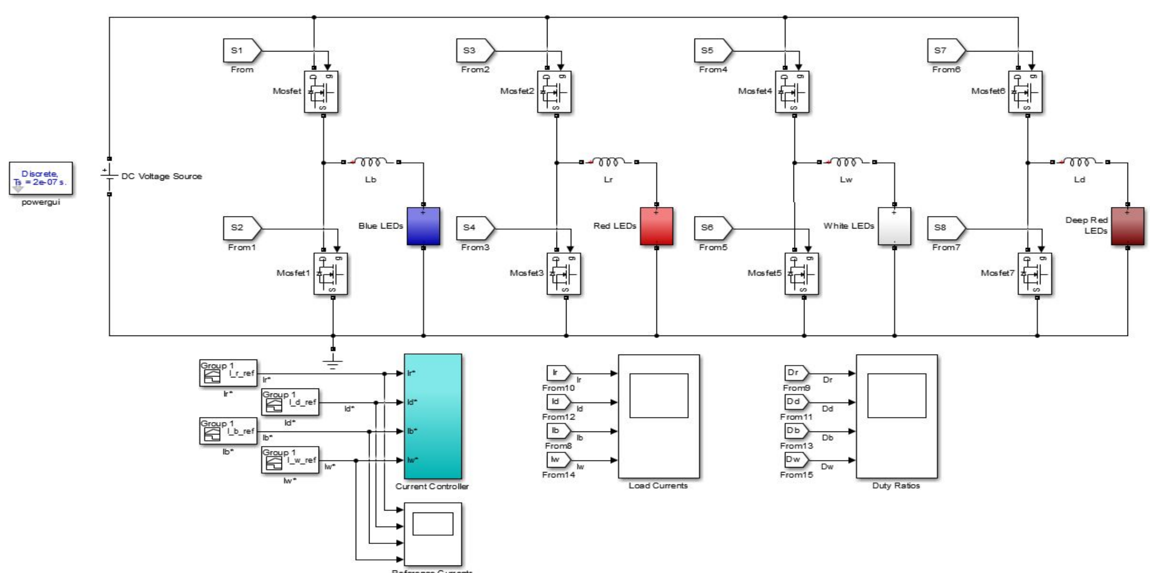

Figure 6.2: *MATLAB Simulink* model of LED Grow-light System

(The output filter capacitors have been embedded in the LED blocks)

6.3 Challenges in Simulation

The model of diode in *MATLAB Simulink* is built to suit the characteristics of an ideal switch. Hence, when that model simulates turn ON and OFF characteristics, it ramps up the current with almost infinite slope. This can be seen in the simulation results shown below when the simulation for the Grow-light system was done using diode models with modified parameters to imitate LEDs:

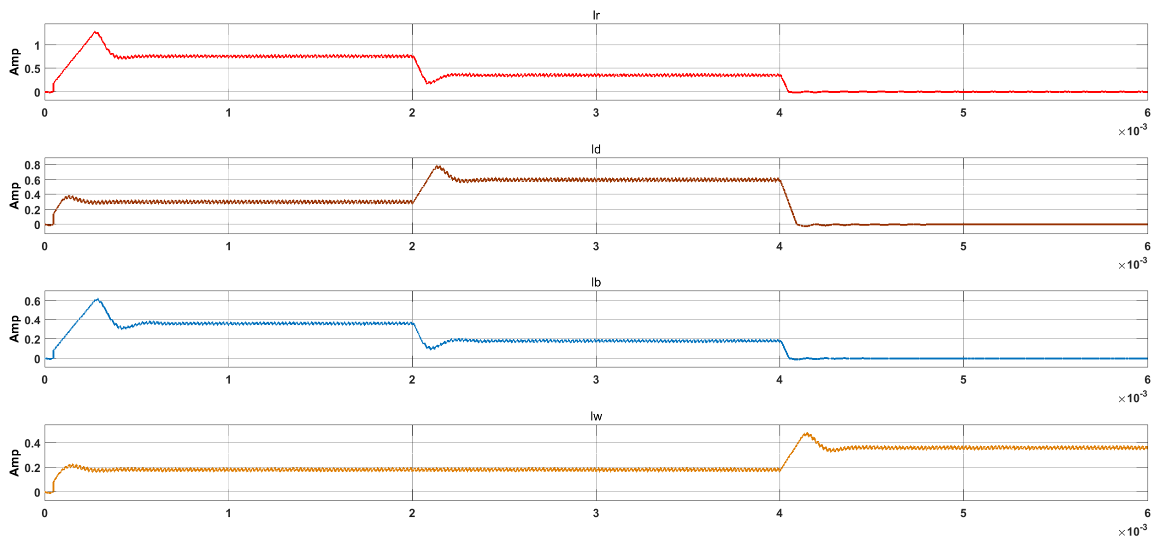

Figure 6.3: Simulation Results: Load Current with LED Model

From the figure it can be seen that the current rises and falls with a slope different than the slope of the inductor current and hence, the filter capacitor gets completely bypassed when the ideal switches turn ON causing the entire ripple current to flow through the LEDs.

We are working on making a better model of LEDs in *MATLAB Simulink* using controlled current source, current dependant voltage source etc. based on the diode-equation model of LEDs. Some research has been done and published on LED modeling and optimization of N x M configuration of LEDs[14].

To mitigate the issues with the diode models in *MATLAB Simulink*, a resistive load equivalent to the LED steady state resistance was used for generating simulation results. This helps to check if the output filter capacitor is filtering the required current ripple out and the load is supplied a current with ripple within the preset tolerance.

6.4 Simulation Results

Following are the simulation results for 3 step changes in reference inputs to the current controller in simulation of the system using the LED steady state resistance as load:

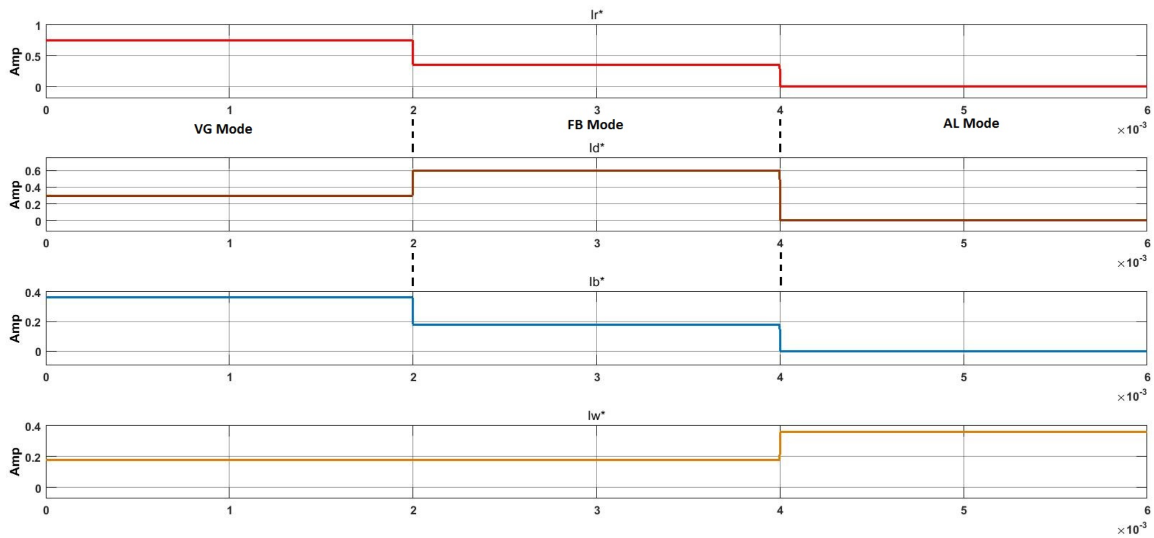

(a) Current Reference

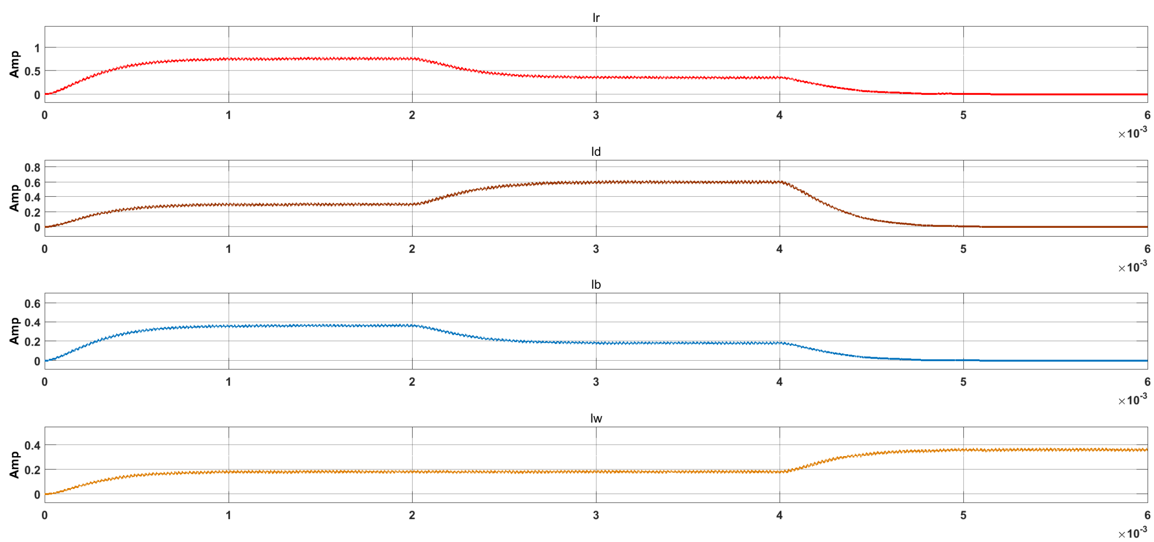

(b) Load Current

Figure 6.4: Simulation Results: Load Current with Resistive Load

In the above figure, reference currents corresponding to the 3 modes of lighting for 4 channels are viz. I_r^*, I_d^*, I_b^* and I_w^* respectively and load currents corresponding to the 3 modes of lighting for 4 channels are viz. I_r, I_d, I_b and I_w respectively for Red, Deep Red, Blue and White light.

Chapter 7

Experimental Studies

7.1 Hardware System Description

Following assumptions were made before designing the hardware:

1. No on board power supplies have been used as power sources for the converter and various ICs. All power supplies are externally connected.

2. No isolation between signal and power ground has been designed since it is not required for proof of concept.

Following diagram describes the system hardware for one channel of the LED Grow-light system:

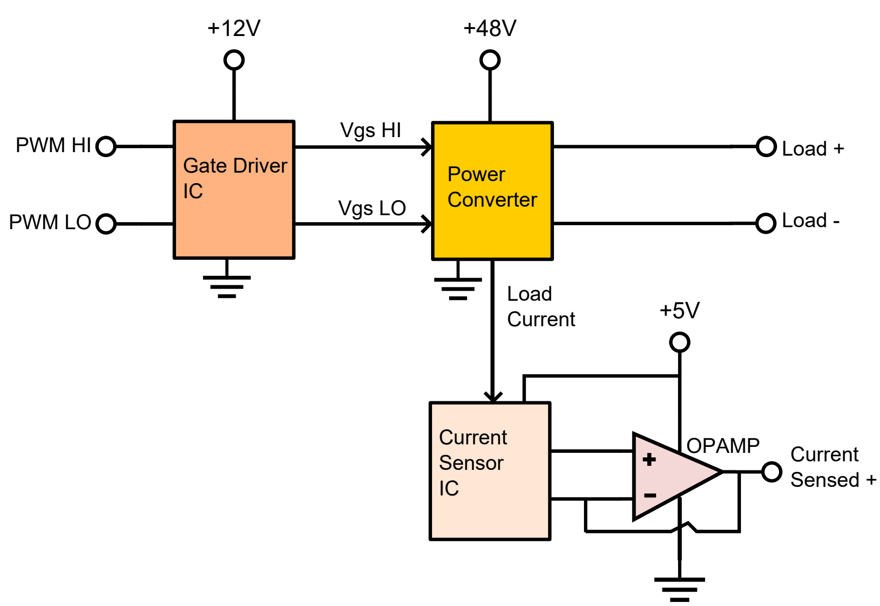

Figure 7.1: System Hardware Block Diagram for 1 Channel

7.2 Selection of Various Components for Hardware

7.2.1 Selection of Passive Components

Although the synchronous buck converter design described in section 5 establishes the minimum inductance and capacitance needed to keep the current ripple in check, the exact value of inductance and capacitance isn't always available with manufacturers. Hence inductors and capacitors with values of inductance and capacitance close enough to the design have been chosen for hardware implementation. Following are the values of L and C that have been used for the hardware implementation:

Channel	**Color of Light**	$L(mH)$	$C(nF)$
1	Red	4	100
2	Deep Red	4.7	100
3	Blue	6.8	100
4	White	6.5	100

Table 7.1: Passive Components for Hardware

7.2.2 Selection of MOSFETs

For hardware implementation, N-Channel FDB2552 MOSFETs manufactured by *Fairchild Semiconductor* have been used. Following are the significant characteristics of the chosen MOSFETs:

- Power Rating - 150V, 37A
- $r_{DS}(ON)$ - 32 $m\Omega$
- Total Gate Charge (Q_{gtot}) - 39 nC
- Low Miller Charge

7.2.3 Selection of Gate Drive

Since the DC-DC power converter topology is based on synchronous buck converters, we need a gate drive that has the following characteristics:

1. High Side Switch Driving Capability
2. Low Side Switch Driving Capability

3. Single Chip Drives both High and Low Side Switch

A 2 input - 2 output, 120 V Boot HF High Side and Low Side Driver manufactured by *Texas Instruments* was used in the hardware implementation. Following are the significant characteristics of the chosen gate driver:

- TTL compatible input pins can tolerate -10 V to +20 V independent of V_{DD}
- Typical V_{DD} - 5 V to 17 V
- Fast propagation delay time (20 ns)
- Drives high and low side switch using a boot-strap circuit

7.2.4 Selection of Current Sensor

Since the output current of the converter directly affects the PPFD generated by the LEDs, it is extremely important to make sure that the current is accurately measured from the output side of the converters so that the feedback control system is able to track the reference inputs set by the user. A hall-effect based sensor ACS723 manufactured by *Allegro Inc.* was used in the hardware implementation. Following are the significant characteristics of the chosen current sensor:

- Pin selectable bandwidth - 20 to 80 kHz
- 0.65 $m\Omega$ primary conductor resistance for low power loss and high inrush current withstanding capability
- Small footprint, low profile SOIC-8 package
- Integrated shield eliminated output noise

Since the microcontroller used for current control is placed away from the current sensor IC, a cable has to be used to tranmit the analog signal which might catch noise along the length of cable. To counteract the noise and give a pure DC voltage output to the ADC proportional to the measured current, a buffer with a simple non-inverting OPAMP circuit with a *Texas Instruments* TLV2470A OPAMP is added next to the current sensor.

7.2.5 Selection of LEDs

Since the lead times on the *EverlightInc*. LEDs was exceptionally long following LEDs with similar forward voltage bins as the design previously described were selected for hardware implementation of the LED Grow-light system:

Channel	**LED Color**	$V_f(V)$
1 and 2	Red	2.2
3 and 4	Green	3.3

Table 7.2: Selection of LEDs for Hardware

For testing the hardware implementation, a PCB was made with N x M configuration of LEDs without considering the uniform distribution of light. Following is image the LED PCB designed for testing the hardware implementation of the LED Grow-light system:

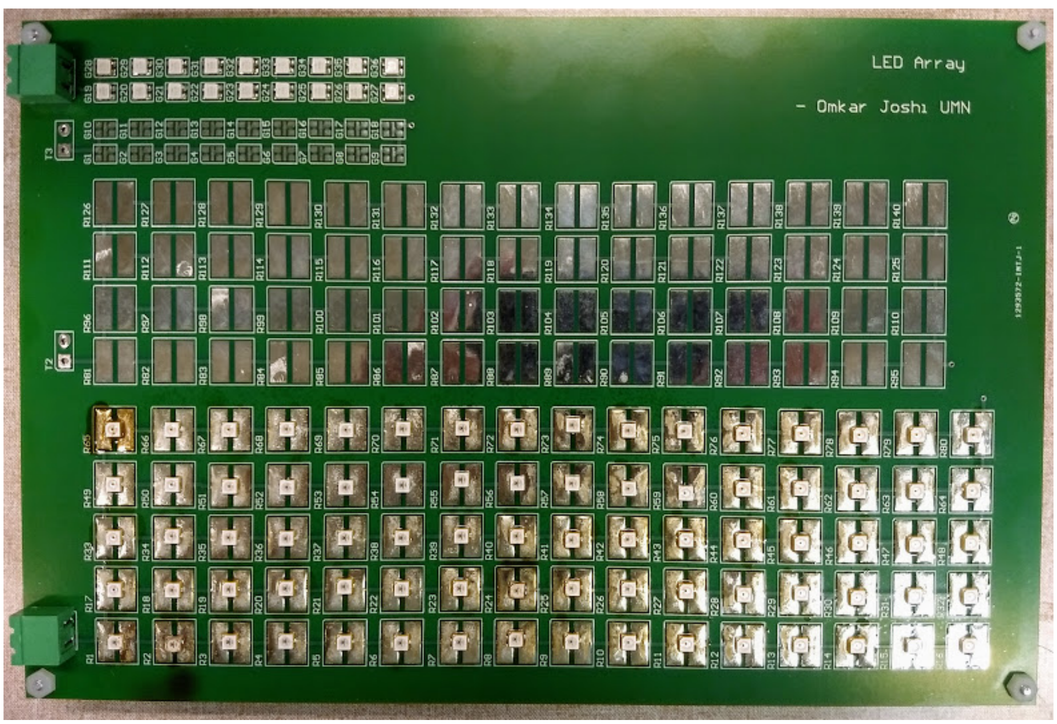

Figure 7.2: PCB with N x M Configuration of LEDs

7.3 PCB Design

PCB design for the DC-DC power converter was done using *Altium*17.1. Following is the list of connectors used:

Connector	Function
Shrouded 10 pin header	PWM input to the gate driver IC
2 pin headers (90°)	Terminals for 48 V DC and load
Male barrel connector	5 V DC for current sensor and OPAMP IC
Male barrel connector	12 V DC for gate driver IC
SMA female connector	Terminal for analog output of current sensor

Table 7.3: List of Connectors for 1 Channel

7.3.1 Schematic Diagram

Following the schematic diagram of one channel of the DC-DC power converter with the current sensor and OPAMP:

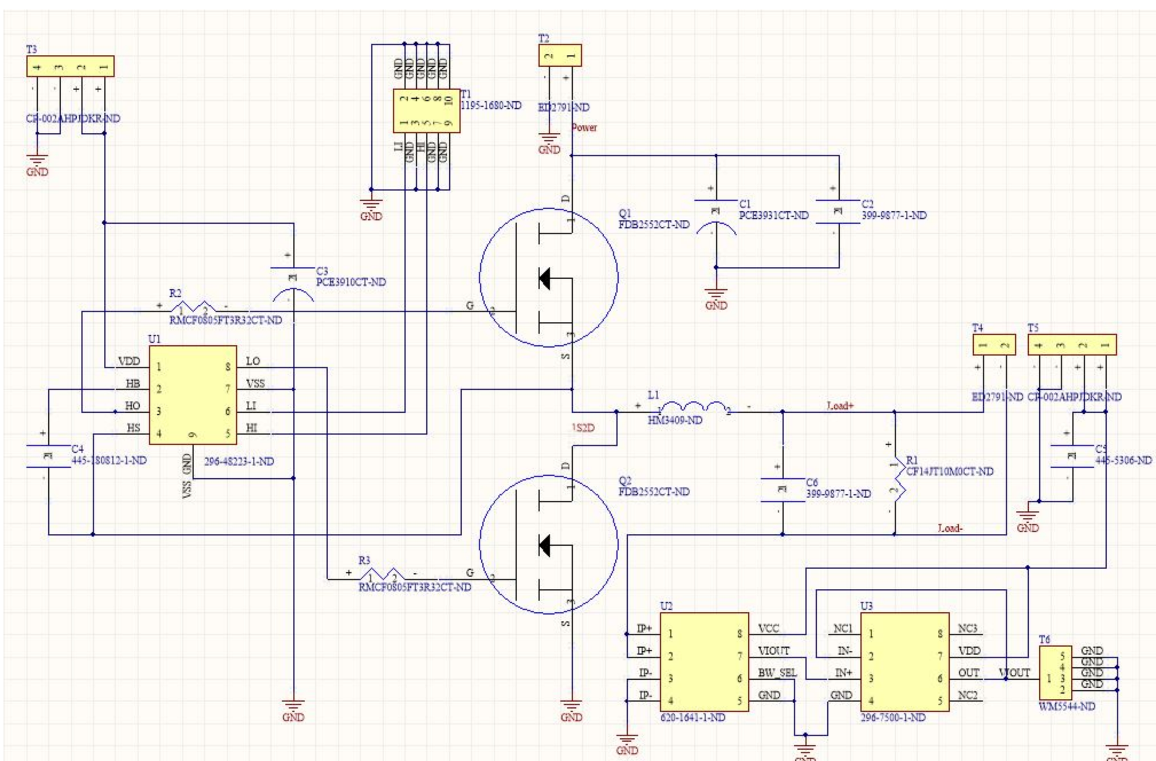

Figure 7.3: Altium PCB Schematic for 1 Channel

7.3.2 PCB Layout

A 2 layer PCB was designed for the hardware implementation of DC-DC power converter with current sensor. Considering both assumptions mentioned in section 7.1, bottom layer of the PCB was used as ground for all the component. A copper layer pour was designed for the entire gorunding layer in order to reduce the i^2R power loss.

Following images show the PCB layout for one channel of the DC-DC power converter with the all the active and passive components along with the connectors used:

1. Altium PCB layout
   Following is the top layer of the PCB layout designed in *Altium*17.1:

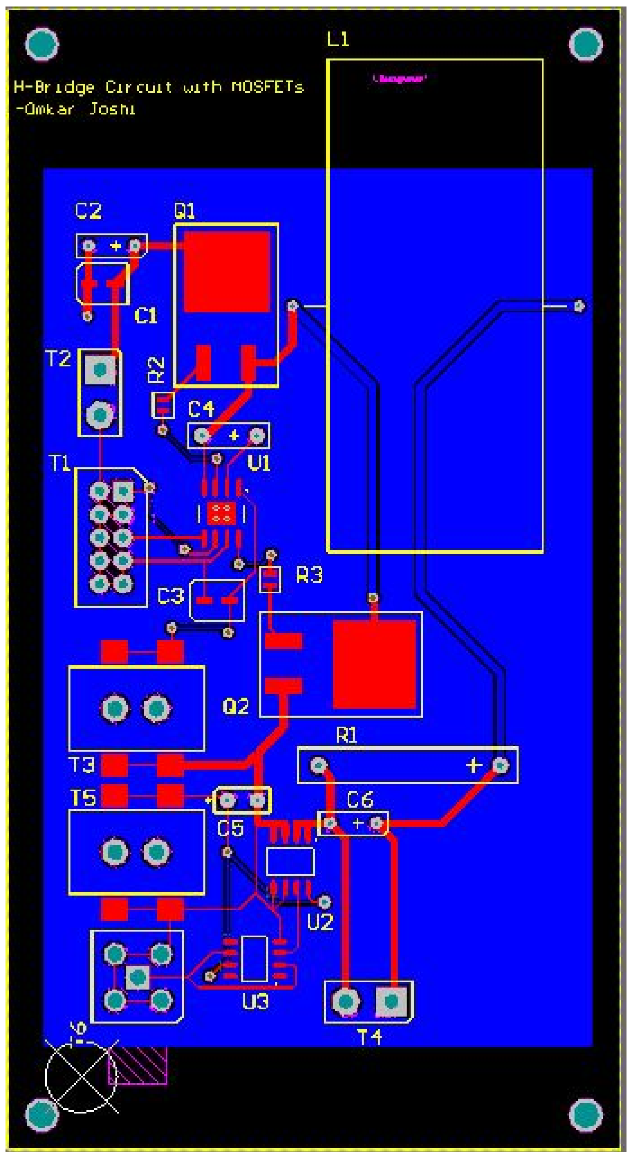

Figure 7.4: Altium PCB Layout for 1 Channel

2. Fabricated PCB with 2 layers and 1 oz. copper on FR4

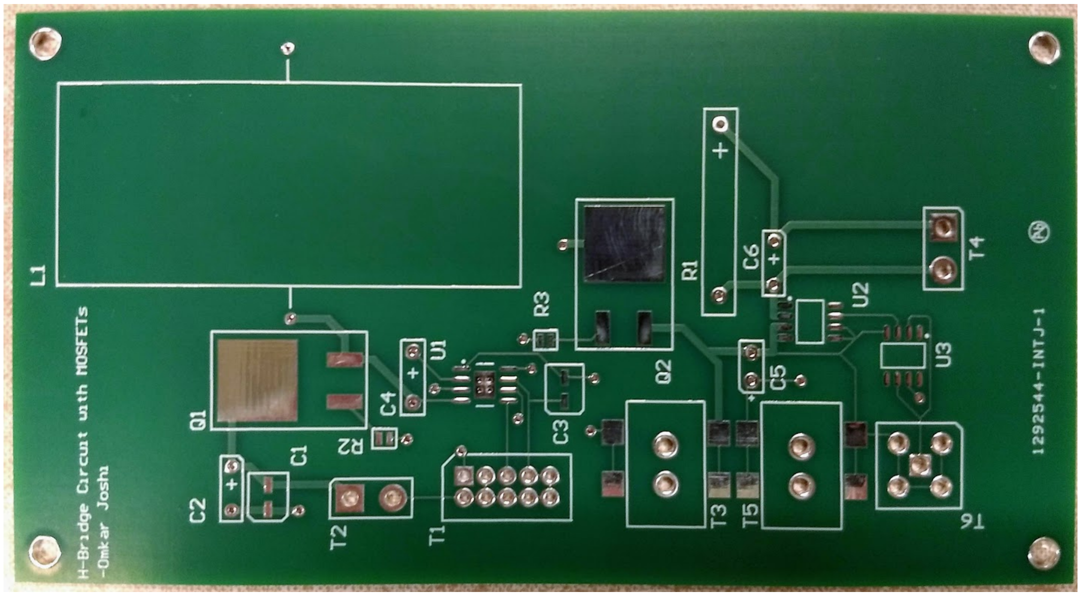

Figure 7.5: Fabricated PCB for 1 Channel

3. Assembled PCB:

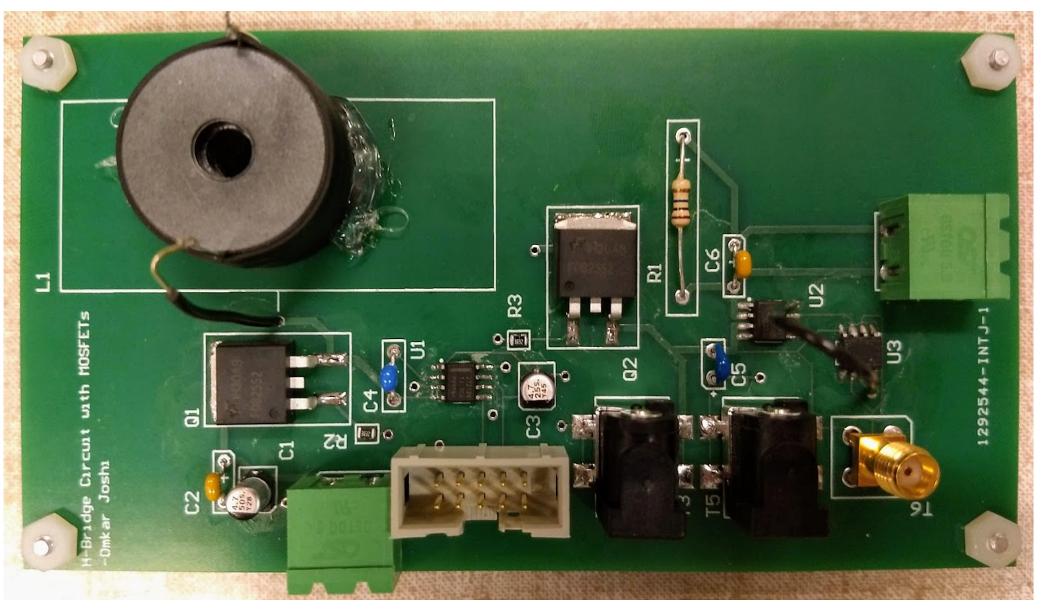

Figure 7.6: Assembled PCB for 1 Channel

7.4 Selection of Micro-controller and Software

A *Texas Instruments* DSP board with multiple PWM channels and ADCs was used as the main hardware controller for this project. It was programmed using *Sciamble Workbench - Version 1* software since it is compatible with the DSP board and *MATLAB Simulink*. Since it doesn't need any changes in the controller design, the PI controllers were easily implemented with it.

7.5 Current References

Since time scale of the simulation is expanded, the results of changing the current references within milli-seconds in simulation are clearly visible. However for hardware implementation, enough time span must be kept within the current references changes to see changes in illumination in real time. The system was subjected to the same 3 lighting modes discussed earlier, with a gap of 5 seconds.

7.6 Controller Design

Since the passive components and LEDs used for hardware implementation of the LED Grow-light system are different than the design described in section 5, the controller gains for satisfying the controller requirements are different than the ones tabulated before. Following table shows the controller gains for all 4 channels of the system:

Channel	**Color of Light**	k_p	k_i
1	Red	0.0738	3.159×10^3
2	Green	0.0961	5.532×10^3

Table 7.4: Hardware: PI Controller Gains for 2 Channels

7.7 Results

7.7.1 Hardware System Setup

Following images show the entire setup for single channels of the LED Grow-light system:

1. DSP Microcontroller Board

Figure 7.7: Hardware Setup: DSP Microcontroller Board

2. Hardware Setup with Resistive Load

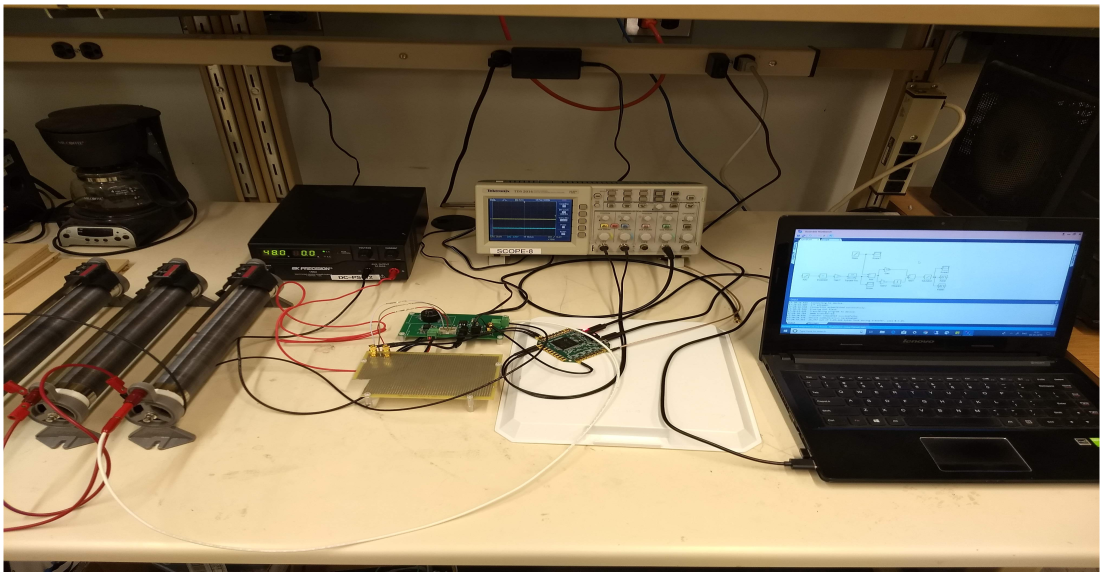

Figure 7.8: Hardware Setup: Resistive Load

3. Hardware Setup with Channel 1 LEDs

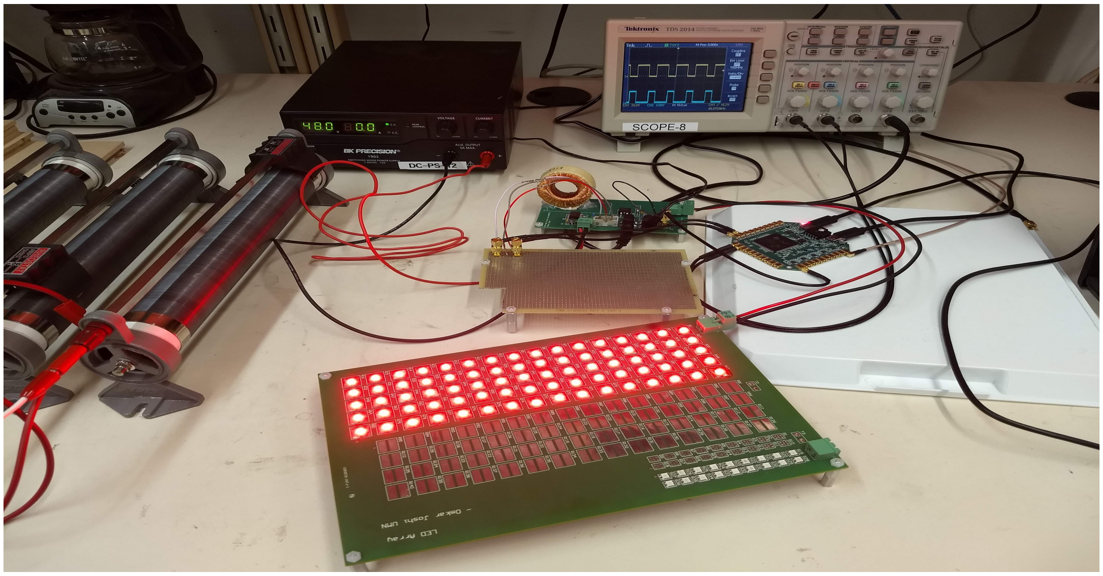

Figure 7.9: Hardware Setup: Channel 1 LEDs

4. Hardware Setup with Channel 2 LEDs

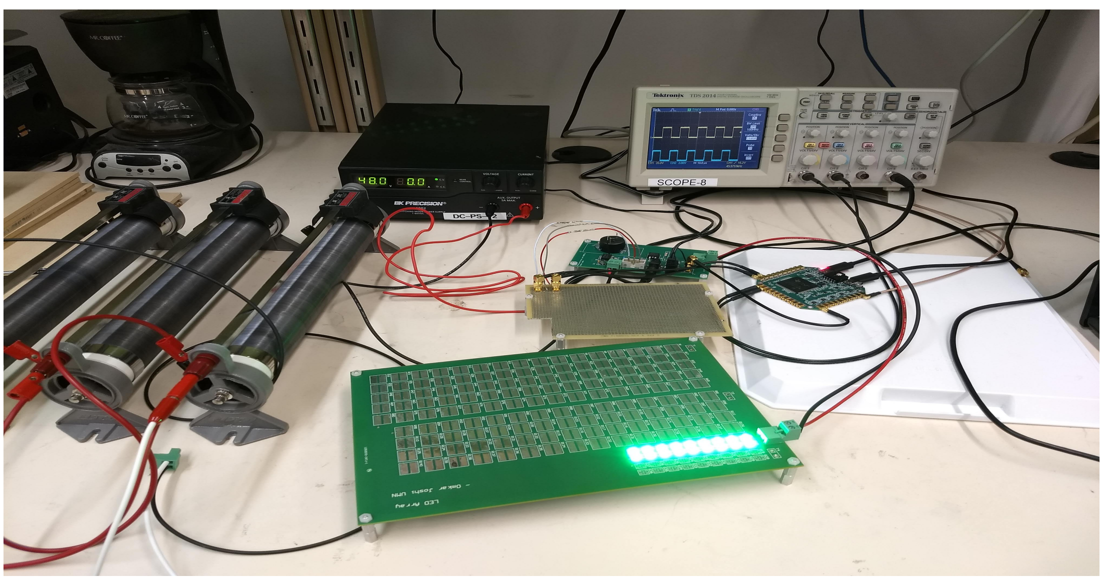

Figure 7.10: Hardware Setup: Channel 2 LEDs

7.7.2 Results with Resistive Load

Following are the results of hardware implementation of the system with equivalent resistive load for 2 channels of the system:

1. Channel 1 : Load Current

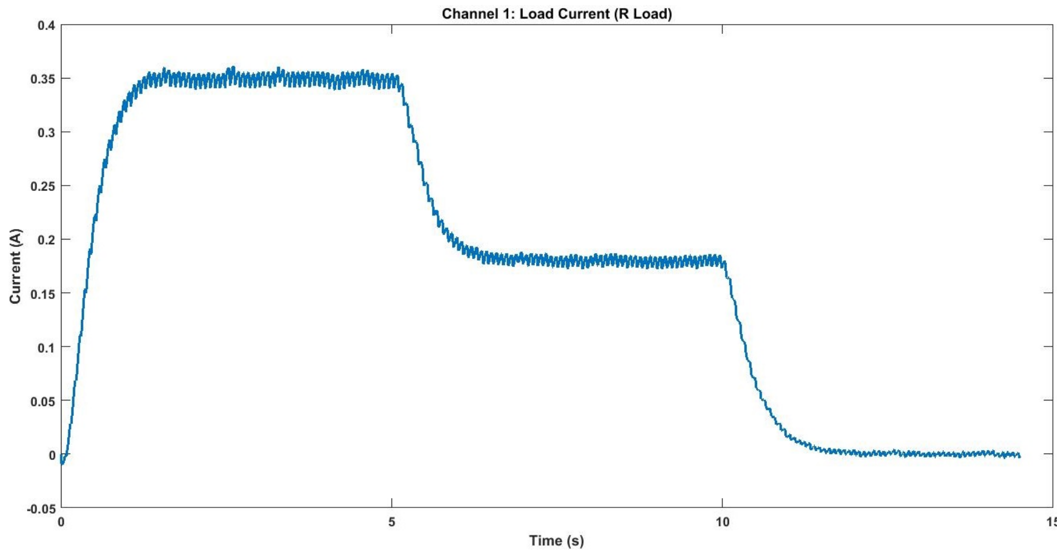

Figure 7.11: Hardware: Channel 1 Load Current (R Load)

2. Channel 2 : Load Current

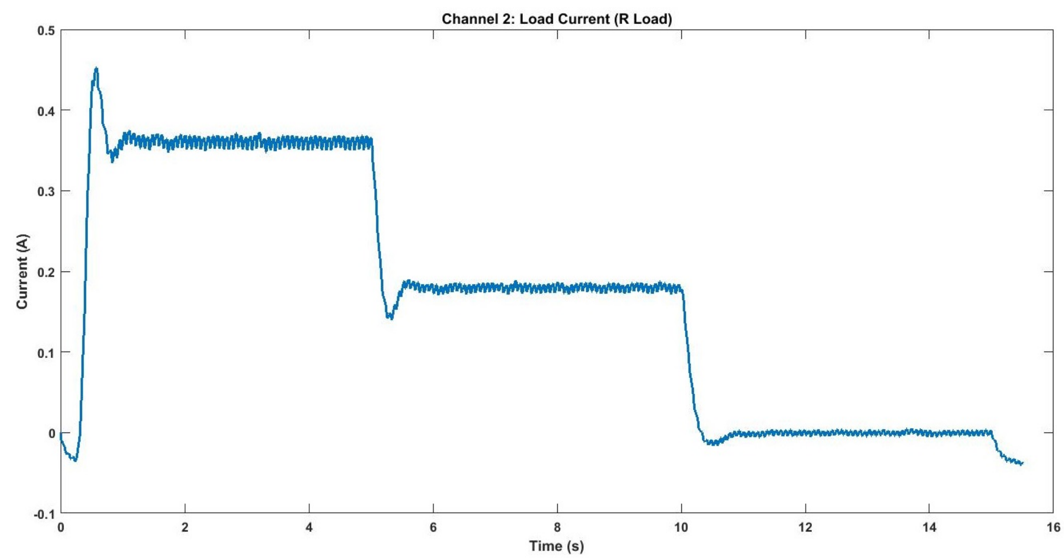

Figure 7.12: Hardware: Channel 2 Load Current (R Load)

7.7.3 Results with LEDs

Following are the results of hardware implementation of the system with LEDs for 2 channels of the system:

1. Channel 1: Load Current

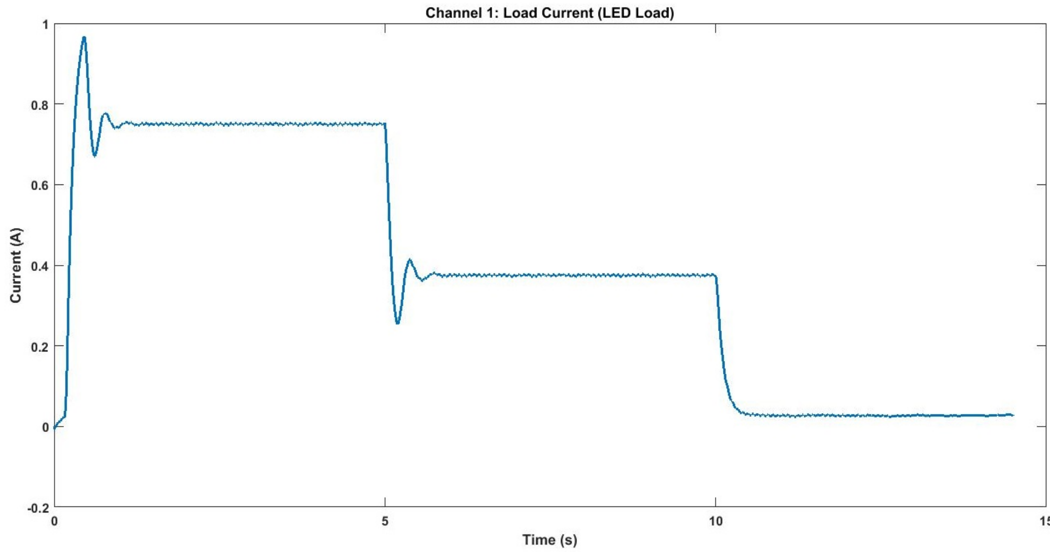

Figure 7.13: Hardware: Channel 1 Load Current (LED Load)

2. Channel 2: Load Current

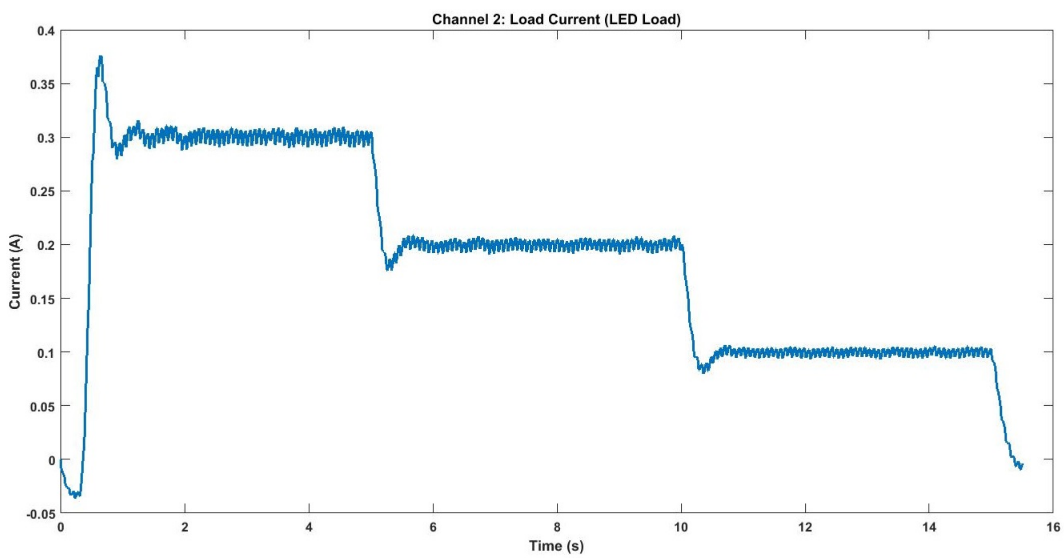

Figure 7.14: Hardware: Channel 2 Load Current (LED Load)

Note: The output of the current sensor was very noisy and thus had to be filtered. However, the proportional gain of the controller has been designed to respond to the measured current signal. Because of the time difference between measured signal and filtered signal, the controller acts faster compared to the change in its reference. Hence there's an overshoot in the converter output.

Chapter 8

Conclusion and Discussion

8.1 Conclusion

The commercially available LED Grow-lights are inexpensive but have poor control over light spectrum and very poor PPFD capacity. The other Grow-lights designed for industrial plant growth face a major issue of compatibility of the commercially available LED drivers with the carefully designed LED arrays and vice-a-versa.
Following has been achieved by the system designed in this project:

1. The system is optimized for simplified control and is modular
2. It ensures more PPFD/LED than most of the commercially available systems
3. It is scalable w.r.t. PPFD capacity and no. of channels for any spectrum of light
4. It has complete and independent control over intensity and spectrum of light generated
5. It is directly integrable with 48 V DC batteries which enables its coupling with PV systems. Hence it can be used anywhere without the requirement of a grid power supply connection.

Hence it can be concluded the designed LED Grow-light system achieves most of the objectives mentioned in the beginning of the thesis.

8.2 Discussion of Future Scope

Although the designed system achieves most of the objectives set, there is scope for future improvement of this system in the following fields:

1. The synchronous buck based DC-DC power converter design can be improved for almost zero LED ripple current with slight tweaks in the passive components used, switching frequency etc. This will greatly improve luminous efficacy and life of LEDs used.

2. Other SIMO topologies based on high frequency transformers, coupled inductors, switching capacitors etc. can be used for designing sophisticated power converters with higher power ratings and better output specifications.

3. LED array can be designed on a multi-layer PCB with same N x M configuration but better LED locations. This will ensure uniform illumination of the plants with the designed panel. Flex PCBs can also be used to make the panels fit in any geometry desired.

4. For the system scaled to industrial level i.e. with a power rating in kW, wide band gap devices like Gallium Nitride (GaN) FETs can be used to reduce size of the circuitry with increased switching frequency and improve efficiency at the same time.

Chapter 9

References

[1] Devesh Singh et al. "LEDs for energy efficient greenhouse lighting". In: *Renewable and Sustainable Energy Reviews* 49 (2015), pp. 139–147.

[2] Neil C Yorio et al. "Improving spinach, radish, and lettuce growth under red light-emitting diodes (LEDs) with blue light supplementation". In: *HortScience* 36.2 (2001), pp. 380–383.

[3] Hyeon-Hye Kim et al. "Green-light supplementation for enhanced lettuce growth under red-and blue-light-emitting diodes". In: *HortScience* 39.7 (2004), pp. 1617–1622.

[4] Wen Huaijiang and Sun Hong. "Backlight LED pulse drive method and luminous efficiency". In: *2012 International Conference on Image Analysis and Signal Processing*. IEEE. 2012, pp. 1–6.

[5] Inc. Fondriest Environmental. *Solar Radiation and Photosynthetically Active Radiation*. 2019. URL: `https://www.fondriest.com/environmental-measurements/parameters/weather/solar-radiation/` (visited on 04/30/2019).

[6] https://www.grobo.io. *How Different Colors of Light Affect Plant Growth*. 2019. URL: `https://www.grobo.io/blogs/grobo/how-different-colors-of-light-affect-plant-growth` (visited on 05/01/2019).

[7] MJ Kasperbauer and DL Karlen. "Plant spacing and reflected far-red light effects on phytochrome-regulated photosynthate allocation in corn seedlings". In: *Crop Science* 34.6 (1994), pp. 1564–1569.

[8] Asuka Yamada et al. "Red: far-red light ratio and far-red light integral promote or retard growth and flowering in Eustoma grandiflorum (Raf.) Shinn". In: *Scientia horticulturae* 120.1 (2009), pp. 101–106.

[9] James E Faust et al. “The effect of daily light integral on bedding plant growth and flowering”. In: *HortScience* 40.3 (2005), pp. 645–649.

[10] Jens Ejury. “Buck converter design”. In: *Infineon Technologies North America (TFNA) Corn Desion Note* 1 (2013).

[11] ON Semiconductor. “LC selection guide for the DC-DC synchronous buck converter”. In: *AND9135/D* (2003).

[12] Ned Mohan. *Power electronics: a first course*. Wiley, 2011.

[13] Qi Xu. “Modeling and Designing of Buck Converters Based on Voltage Mode Control”. In: *Unifying Electrical Engineering and Electronics Engineering*. Springer, 2014, pp. 721–728.

[14] Ray-Lee Lin, Shun-Yao Liu, and Cheng-Jia Tsai. “Optimal LED array combination for dual-loop CCM boost driver”. In: *2012 IEEE Industry Applications Society Annual Meeting*. IEEE. 2012, pp. 1–9.

Appendix A

List of Acronyms and Units

A.1 Acronyms

1. LED - Light Emitting Diode
2. PWM - Pulse Width Modulation
3. PAR - Photosynthetically Active Radiation
4. PFFD - Photosynthetically Active Photon Flux Density
5. DLI - Daily Light Integral
6. PV - Photo Voltaic
7. SIMO - Single Input Multiple Output
8. MOSFET - Metal Oxide Semiconductor Field Effect Transistor
9. CCM - Continuous Conduction Mode
10. PI - Proportional-Integral
11. PCB - Printed Circuit Board
12. IC - Integrated Circuit
13. OPAMP - Operational Amplifier
14. ADC - Analog to Digital Converter

A.2 Units

1. Wavelength - nanometer (nm)
2. PFFD - $\mu mol/m^2 s$
3. DLI - mol/day
4. Current - ampere (A)
5. Voltage - volt (V)
6. Resistance - ohm (Ω)
7. Inductance - milli henry (mH)
8. Capacitance - nano farad (F)
9. Duty Ratio - no unit
10. Frequency - hertz (Hz) and radian/second (rad/s)
11. Magnitude - decibel (dB)
12. Phase - degree ($^\circ$)